NTIA TM-88-135

PROCEDURES FOR CALCULATING FIELD INTENSITIES OF ANTENNAS: PHASE II

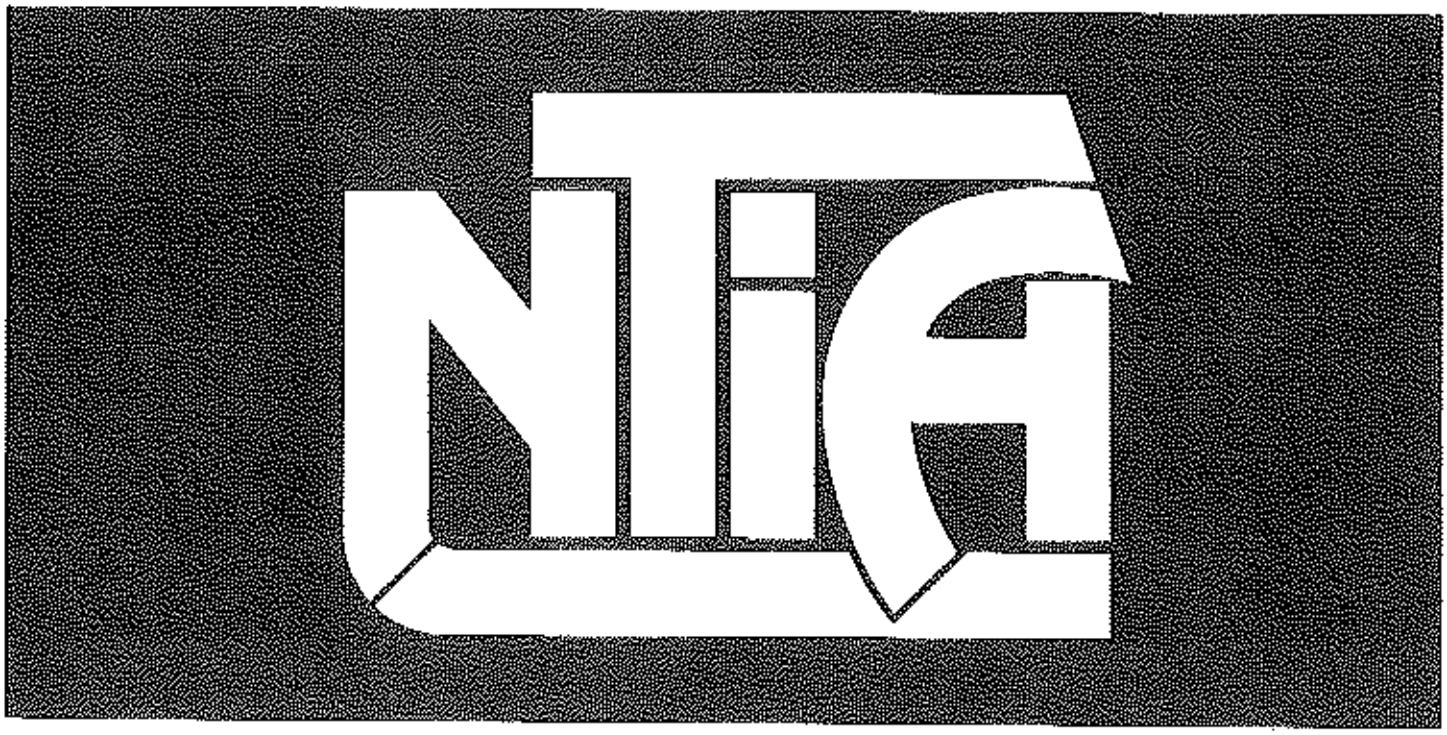

technical memorandum series

U.S. DEPARTMENT OF COMMERCE • National Telecommunications and Information Administration

NTIA TM-88-135

PROCEDURES FOR CALCULATING FIELD INTENSITIES OF ANTENNAS: PHASE II

Herbert K. Kobayashi

Stimulating America's Progress
1913-1988

U.S. DEPARTMENT OF COMMERCE
C. William Verity, Secretary

Alfred C. Sikes, Assistant Secretary
for Communications and Information

SEPTEMBER 1988

TABLE OF CONTENTS

TABLE OF CONTENTS
(continued)

SECTION 3
(continued)

SECTION 4

REFERENCES

TABLE OF CONTENTS
(continued)

LIST OF FIGURES

TABLE OF CONTENTS
(continued)

LIST OF FIGURES
(continued)

LIST OF TABLES

SELECTED LIST OF SYMBOLS

Symbol	Quantity	Page
D	Largest aperture dimension of an antenna (meters)	3-10
D_E	Distance from center to outermost element of a uniform linear array (meters)	3-24
d_A	Normalized distance for an aperture antenna	3-9
d_C	Normalized distance for a corner reflector	3-10
d_W	Normalized distance for a wire antenna	3-9
E	Electric field intensity vector (volts/meter)	3-3
E_F	Far-field E vector (volts/meter)	3-10
E_N	Near-field E vector (volts/meter)	3-10
g_t	Antenna gain referenced to an isotropic source	3-10
H	Magnetic field intensity vector (amperes/meter)	3-3
N	Number of elements in an antenna array	3-24
P_F	Far-field power density (milliwatts/sq-centimeter)	3-10
P_N	Near-field power density (milliwatts/sq-centimeter)	3-11
p_t	Antenna input power (Watts)	3-10
R	Mainlobe on-axis distance (meters)	3-9
s	Distance from the vertex to the radiator of a corner reflector antenna (wavelengths)	3-26
λ	Wavelength in freespace	3-5
Φ_{CR}	Included angle of a corner reflector antenna	3-26

SECTION 1

INTRODUCTION

BACKGROUND

The National Telecommunications and Information Administration (NTIA) is responsible for managing the Federal Government's use of the radio frequency spectrum. NTIA's responsibilities include establishing policies concerning spectrum assignment, allocation and use, and providing the various departments and agencies with guidance to ensure that their conduct of telecommunications activities is consistent with these policies.[1]

This report, its predecessor NTIA TM-87-129,[2] and its microcomputer implementation,[3] address the need for simple, easy-to-use procedures to assess whether a federal agency's use of the RF spectrum will conform to RF radiation criteria. Operators of federal radio communications systems and NTIA, the authority on a federal agency's use of the RF spectrum, will benefit from these procedures.

In the earlier report, conservative estimates of the on-axis near-field power density were found for antenna types listed in the Government Master File (GMF) by using data normally supplied by federal agencies on Form NTIA-35, "Antenna Equipment Characteristics," and manufacturer's specification sheets. Power density is calculated from simple formulas and correction factors obtained from normalized curves. The curves are predetermined for hand-calculation procedures in Reference 2. In the menu-driven Antenna Field Intensity (AFI) Program, the curves are generated, as required, by coded algorithms and entail no hand calculations.

OBJECTIVES

The specific objectives of this report were to:

1. extend the on-axis near-field coverage of antenna types listed in the GMF,

---

[1] NTIA, *Manual of Regulations and Procedures for Federal Radio Frequency Management*, U.S. Department of Commerce, National Telecommunications and Information Administration, Washington, D.C., Revised May 1988.

[2] A. Farrar and E. Chang, *Procedures for Calculating Field Intensities of Antennas*, NTIA Report TM-87-129, U.S. Department of Commerce, September 1987.

[3] E. Calhoon and H. K. Kobayashi, "Antenna Field Intensity (AFI) Program," NTIA, Annapolis, unpublished.

2. provide additional guidance in applying procedures for finding the near-field power density,

3. examine the feasibility of using simple models to calculate the off-axis near-field power density of wire and aperture antennas, and

4. incorporate the additional antennas of the on-axis near-field analysis into the AFI Program.

APPROACH

To accomplish the aforementioned objectives, the following tasks were undertaken.

1. The GMF was resurveyed for additional antenna types and sorted to confirm the criteria for placement of antennas into wire and aperture categories.

2. The published literature was searched for methods suitable for off-axis analysis, and for analytical solutions and measured data required to verify the numerical computations of (3) below.

3. The near-field on-/off-axis behavior of several generic antenna types was clarified with the aid of numerical computer programs, and the findings incorporated into this report and the enhancement of the AFI Program.

SECTION 2

GENERAL SUMMARY AND RECOMMENDATIONS

GENERAL SUMMARY

The objectives of this report listed in Section 1 have been met by:

1. extending on-axis near-field power density procedures to encompass 97% of the GMF antenna types analyzed here,

2. providing guidance and additional formulas for selecting an antenna type from an augmented total of more than 20 choices,

3. clarifying the two broad overlapping categories of antennas: wire or linear and aperture, as a prelude to on-axis mainlobe antenna selection and mainlobe off-axis numerical computation, and

4. incorporating the additional antennas addressed in this report into the on-axis near-field algorithms of the AFI Program.

The objective of calculating off-axis power density has been partially met by providing procedures for analyzing two widely-different antennas by using numerical computer programs.

RECOMMENDATIONS

The following are NTIA staff recommendations based on the technical findings contained in this report. NTIA management will evaluate these recommendations to determine if they can, or should, be implemented from a policy, regulatory, or procedural viewpoint. Any action to implement these recommendations will be accomplished under separate correspondence by modification of established rules, regulations, or procedures. It is recommended that the following be done by NTIA.

1. The procedures in this report and its predecessor, TM-87-129, should be used when calculating the near- and far-field intensities of a Federal Government antenna.

2. Specific procedures for assessing the off-axis field intensity of important antenna types, starting with the parabolic reflector antenna, should be investigated, since a general procedure for off-axis analysis was not found.

SECTION 3

ADDITIONAL ANTENNAS FOR ON-AXIS ANALYSIS

DATA BASE FOR SELECTING ANTENNAS

The GMF, an NTIA frequency assignment data file of government telecommunication systems, has been reexamined and presented in a form which complements the original antenna table (Reference 2, p. 3-3) and provides additional data for characterizing a transmitting antenna (TABLE 3-1).

An examination of the old and new GMF table can help in determining whether an antenna is in the linear (wire) or aperture radiator category. This is the first step in the PC procedure for finding the field intensity, which is explained in greater detail at the end of this section. In Reference 2, aperture antennas were described as high gain (> 18 dBi) high frequency (> 1.2 GHz) radiators. This generalization can be verified by comparing antenna type against the FREQ and GAIN columns in TABLE 3-1 where linear antennas are seen to have high percentages.

Several antenna types can be constructed with thin rods or alternatively with sheet metal in the transitional UHF range of 0.3 to 3.0 GHz making them difficult to place as linear or aperture. Since each is less than one percent of the total number of government antennas, they are excluded as types for analysis. Typically they are broadband low-gain radiators; *vis-a-vis* the biconical, conical, helix, and traveling wave antennas.

The three categories of antennas discussed above (wire, aperture, and broadband) are identifiable in practice. For a modern treatment comparing and contrasting these antennas, see Stutzman and Thiele 1981, Chapters 5, 6, and 8.[4]

ANTENNA TYPES SELECTED FOR ANALYSIS

The antenna types chosen for augmenting the earlier Procedures and implementation on the PC disk are identified by a plus sign + in TABLE 3-1. With their inclusion, close to 97% of the 100,000 transmitting antennas and antenna types with number greater than 600 are now represented.

In alphabetical order the antenna types are:

Coaxial (dipole)	Folded dipole
Corner reflector	Ground plane
Dipole array	Omnidirectional
Discone	Stacked array
	Stub (blade)

[4] Stutzman, WL., and G.A. Thiele, *Antenna Theory and Design*, J. Wiley & Sons, New York, N.Y. 1981.

TABLE 3-1

CATEGORIZATION OF TRANSMITTING ANTENNAS USED BY THE MAJORITY OF GOVERNMENT TELECOMMUNICATION SYSTEMS

Source: Government Master File (GMF), July 1987

ANTENNA TYPE from GMF file	NUMBER ant. type	PCT of Total Number	FREQ <1.2 GHz Pct of type number	GAIN <18 dBi Pct of type number
Biconical	182	< 1	0	100
+Blade	1852	2	87	100
Broadband	566	< 1	100	100
Cardioid	194	< 1	99	99
Cassegrain	35	< 1	100	6
+Coaxial (dipole)	2028	2	100	100
*Colinear	26559	25	100	100
Conical	52	< 1	63	not avail.
+Corner reflector	2737	3	100	100
*Dipole	9930	10	98	99
+Dipole array	2994	3	99	92
+Discone	3150	3	not avail.	100
Folded Coaxial	134	< 1	100	100
+Folded Dipole	1065	1	100	100
+Ground plane	5678	6	100	100
Helix	348	< 1	66	82
*Horn	881	1	4	48
*Log periodic	832	1	100	42
Loop	54	< 1	93	96
Microstrip	46	< 1	0	100
*Monopole	1479	1	90	100
+Omnidirectional	661	1	99	100
*Parabol reflect	18759	18	5	3
Phased array	179	< 1	20	9
Pillbox	240	< 1	83	100
Planar array	103	< 1	not avail.	not avail.
Rhombic	231	< 1	100	100
Slotted array	364	< 1	not avail.	not avail.
+Stacked array	974	1	97	96
+Stub	619	< 1	61	100
Swastika	119	< 1	100	100
Traveling wave	167	< 1	100	51
*Vertical dipole	902	1	99	100
*Vertical radiat	749	< 1	98	99
*Whip	10580	10	100	100
*Yagi\Yagi array	6530	6	100	100
TOTAL NUMBER:	101972			

*Indicates antenna types considered in Reference 2.
+Indicates antenna types considered in this report.

These in turn can be grouped into basic types as follow.

Vertical half-wave dipole:	Folded dipole Coaxial (dipole)
Vert. quart.-wave at ground plane:	Stub (blade) Ground-plane Omnidirectional
Broadband omnidirectional:	Discone
Linear arrays of dipoles:	Dipole array Stacked array
Dipole with plane reflectors:	Corner reflector

After a discussion on the methods employed for calculating the near-field intensity of radiators, the basic types will be taken up in the order listed above.

METHODS FOR OBTAINING ON-AXIS NEAR-FIELD INTENSITIES

Introduction

The overriding consideration when describing radiation at any distance from an antenna is the very different behavior of the electric and magnetic vectors in the near- and far-fields (Figure 3-1). Even for linear antennas where the far-field vectors are linear and orthogonal, in the near-field the vectors are generally ellipses and are non-orthogonal. Consequently, the intrinsic impedance varies spatially and is not a constant 377 ohms as often assumed in the far-field. Also, the E and H vectors have radial components near the antenna, which are absent or negligible in the far-field.

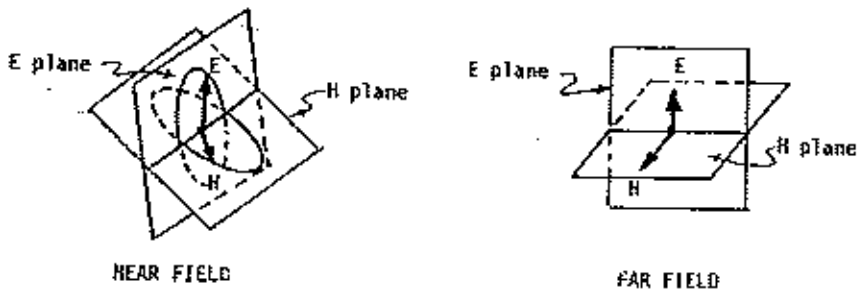

Figure 3-1. E and H vectors in the near- and far-field of a typical antenna.

A graphical depiction of how an ellipsoidal vector changes with position may be found on page 261 of *Near Fields of Thin-Wire Antennas-Computation and Experiment*.[5] The separation of distance into near- and far-fields, crucial to the application of this report, is also discussed and defined for linear or wire antennas. This is important since the large majority of GMF antennas are linear.

Two numerical computer codes were utilized for on-axis near-field intensity calculations: MININEC (Mini-Numerical EM Code) Version 3 and NEC-BSC (Numerical EM Code-Basic Scattering Code) Version 2.[6,7] The first is an integral equation method-of-moments code for wire radiators, and the second treats structures composed of flat plates by asymptotic techniques based on the Geometrical Theory of Diffraction.

In this section, numerical codes are applied specifically to the on-axis situation. The application of codes to off-axis analyses is taken up in Section 4.

MININEC Code Applied to Wire Antennas

The MININEC code was run to obtain near-field data for all antenna types excluding the corner reflector. This PC implementable code is basically similar to the Numerical Electromagnetic Code (NEC) employed in the earlier Procedure (see Reference 2, pages 4-7 and 4-9) in being a moment method applicable to wire conductors. Both codes find numerical solutions to integral equations representing the E and H fields generated by currents in wires. An important restriction is that wire radius must be very small compared to segment length by about two orders of magnitude.

MININEC and NEC differ in other ways. From its inception, the former was designed for the desktop computer with the practicing Electromagnetic (EM) designer in mind. It is a true computer-aided engineering (CAE) tool often found associated with circuit design software.[8] For readable succinct introductions of the MININEC

---

[5] Adams, A.T., T.E. Baldwin, and D.E. Warren, *Near Fields of Thin-Wire Antennas-Computation and Experiment*, IEEE Transactions on Electromagnetic Compatibility, vol. EMC-20, no. 1, pp. 259-266, February 1978.

[6] Logan, J.C., and J.W. Rockway, *The New MININEC (Version 3): A Mini-Numerical Electromagnetic Code*, Naval Oceans Systems Command, San Diego, CA 92152, NOSC TD 938, September 1986.

[7] Marhefka, R.J., and W.D. Burnside, *Numerical Electromagnetic Code - Basic Scattering Code NEC-BSC (Version 2) Part I: User's Manual and Part II: Code Manual*, The Ohio State University ElectroScience Laboratory, Department of Electrical Engineering, Columbus, OH 43212, December 1982.

[8] Li, S.T., et al., *Microcomputer Tools for Communications Engineering*, Artech House, Inc., Dedham, MA 1983.

approach to antenna and transmission line problems, see two articles by D.V. Campbell.[9]

MININEC obtains the three vectors that define the intensity at a point by finding the electric field strength induced in a virtual dipole .001 long which is positioned sequentially in the x, y, and z directions (see Reference 6, pp. 15-17). The most important calculation is the peak or maximum field intensity for the E or H vector; however, the average value may also be obtained from angular output data.

Only free-space and a perfectly conducting half-space can be simulated for near-field calculations with MININEC. Even so, close comparisons can be obtained with field measurements of simple antennas over good conducting surfaces. For example, Figure 3-2 displays MININEC calculation versus measured data for a typical simple antenna problem (see Reference 6, p. 52). The curves are nearly identical except at distances greater than a tenth wavelength where the sensor was affected by nearby structures. The segment number (a MININEC input parameter) is the number of pieces in a spatially specified thin-wire conductor. Modeling accuracy increases with segment number; unfortunately this trend is countered by an unavoidable geometric increase in CPU processing.

NEC-BSC Code Applied to Aperture Antennas

When the number of segments and attendent increase in CPU time becomes excessive in MININEC and similar thin-wire approximation codes, a different computational method must be considered. Ohio State University's Numerical Electromagnetic Code - Basic Scattering Code (NEC-BSC) complements the wire codes by its ability to model dielectric and conducting slabs and elliptic cylinders at upper-VHF and above. The thin-wire approximation is best applied to linear conductors at lower VHF and below.[10] NEC-BSC is not a combination code as the name implies, but is based on the Geometrical Theory of Diffraction and uniform asymptotic analysis rather than the method-of-moments.[11,12]

---

[9] Campbell, D.V., *Personal Computer Applications of MININEC*, IEEE Antennas and Propagation Newsletter, pp. 5-9, February 1984; *Mininec Applications Guide*, Applied Computational Electromagnetics Society Newsletter, pages 21-28, February 1986.

[10] Burke, G.J. and A.J. Pogio, *Numerical Electromagnetics Code (NEC)-Method of Moments, Volume 2* pages 3-6, NOSC Naval Oceans Systems Center, San Diego, CA NOSC-TD 116, January 1981.

[11] Burnside, W.D., *Computer Modeling of Electromagnetic Problems Using the Geometrical Theory of Diffraction*, IEEE International Symposium on Electromagnetic Compatibility, Washington, DC, July 13-15, 1987, pp. 312-316.

[12] Burnside, W.D., R.C. Rudduck, and R.J. Marhefka, *Summary of GTD Computer Codes Developed at the Ohio State University*, IEEE Transactions on Electromagnetic Compatibility, vol. EMC-22, no. 4, pp. 238-243, November 1980.

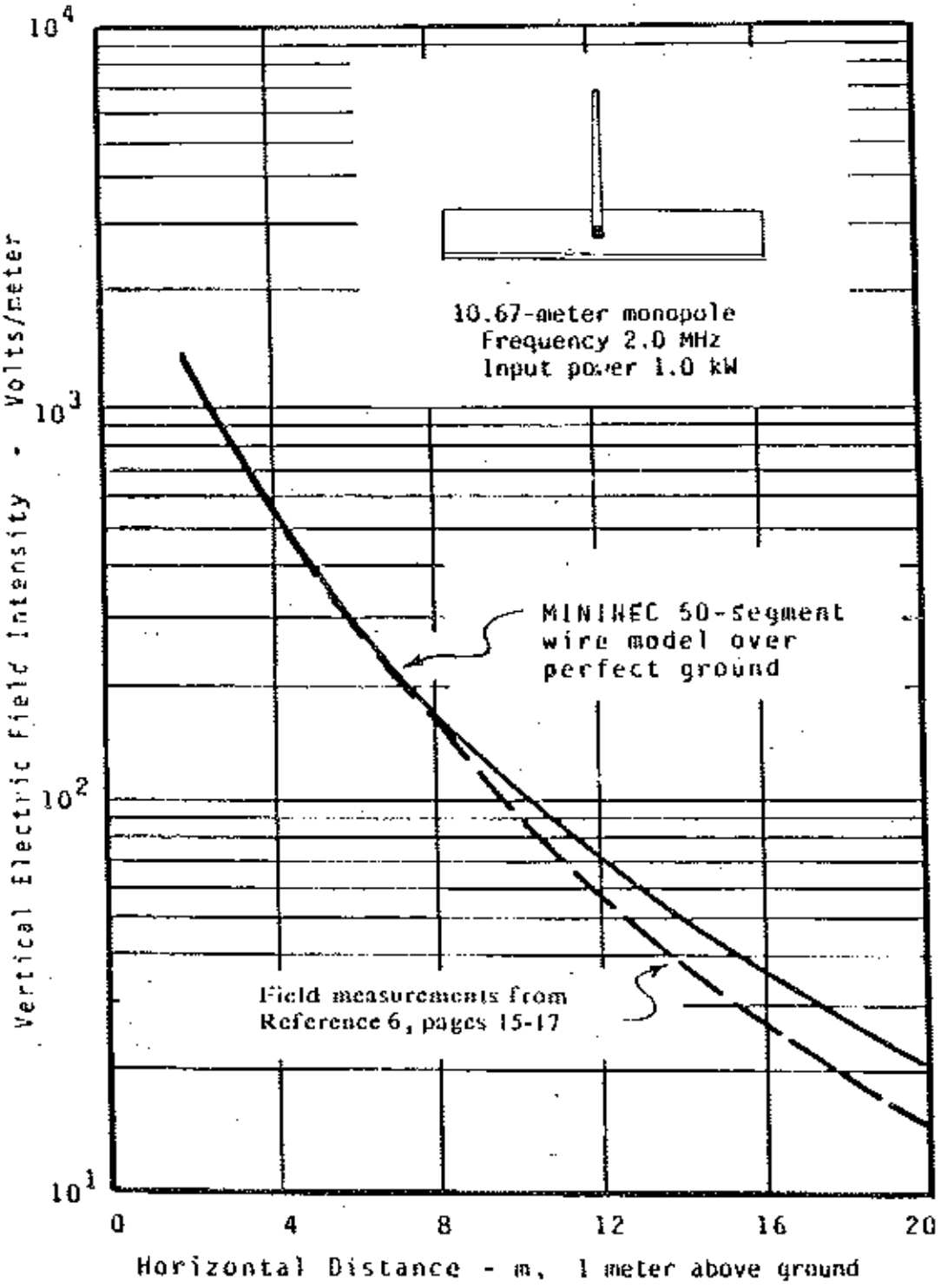

Figure 3-2. Near-field comparison of MININEC calculations and field measurements for a monopole, conducting ground.

NEC-BSC is applied to only one of the additional nine antenna types considered for on-axis near-field analysis: the corner reflector. In order to model a reflector of at least the minimal square-wavelength in aperture area, it would be necessary to have a minimum 300 segments for a wire model. This is well beyond the maximum of 50 for MININEC and 150 for "standard" NEC. The number of acceptable segments can be increased by altering the FORTRAN source code, but the CPU time on a main frame computer would be at least 15 minutes. In contrast, a NEC-BSC run on a VAX-VMS microcomputer for any of the aperture sizes in this report took less than 2 minutes.

ANALYSIS OF ANTENNA TYPES

General Considerations and Calculation of On-Axis Near-Field Intensities

All results for on-axis data were obtained with the MININEC, Version 3, except for those of the corner reflector antenna, which were found with the NEC-BSC, Version 3. As explained earlier, NEC-BSC is very different from MININEC and NEC in theory and can handle problems impractical for the wire codes.

Near-Field Intensity Curves and Normalization Distances for Wire and Aperture Antennas

Near-field intensity and distance from the antenna's electrical center are normalized to their values at a distance considered just within the far-field. Normalization enables an antenna type to be represented by a single curve and to be independent of antenna power input and frequency.

The choice of the nearest far-field distance (hereafter called the normalization distance) is crucial. For wire antennas, this distance is 1.5 wavelengths (1.5λ) and for aperture antennas, it is twice the square of the largest aperture dimension divided by λ. These criteria were chosen to correspond to those in Reference 2. The wire criterion is substantiated for simple radiators by Siarkiewicz, who cautions that complex antennas require method-of-moment computations to establish unique normalization distances.[13] For the aperture criterion, Bickmore and Hansen has a straight-forward account for simple shapes.[14]

Typical correction curves for wire antennas are those found in Figures 3-3 and 3-4. When moving away from a wire antenna, the field intensity generally decreases monotonically. Whatever the behavior in the near field, all curves are asymptotic approaching the normalization distance where the far-field inverse-square relationship takes hold.

---

[13] Siarkiewicz, K.R., *Method of Moments Applications: Near and Far Field Thin-Wire Coupling*, Rome Air Development Center, In-House Technical Report RADC-TR-73-217, vol. IX, January 1976.

[14] Bickmore, R.W. and R.C. Hansen, *Antenna Power Densities in the Fresnel Region*, Proceeding IRE (IEEE), pp. 2119-2120, December 1959.

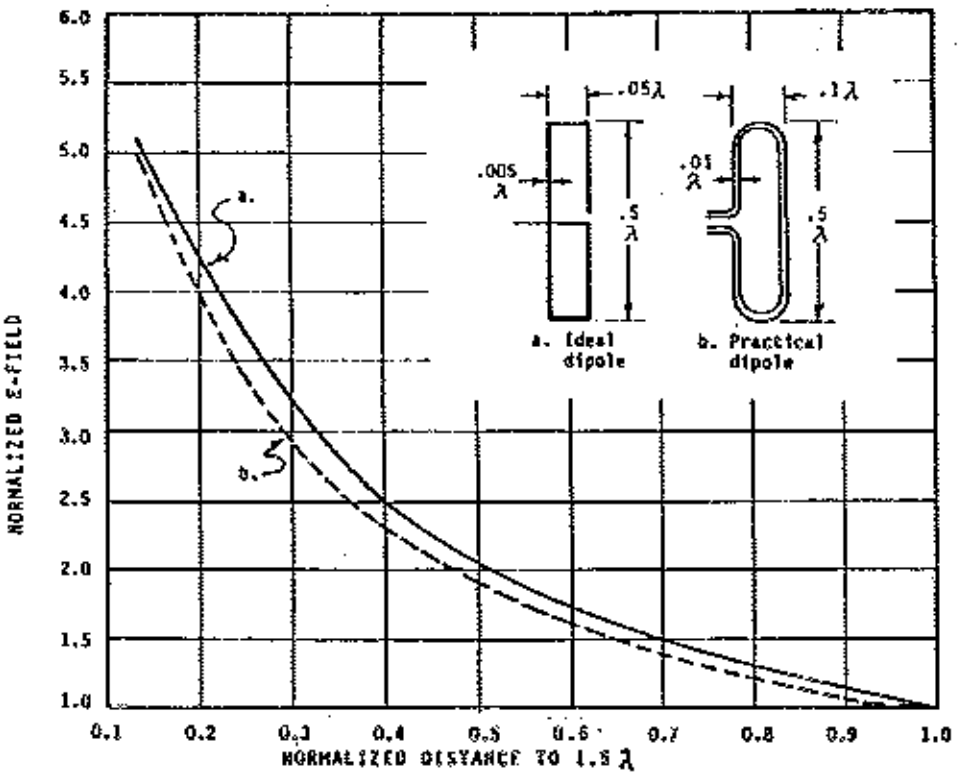

Figure 3-3. Correction factor vs normalized distance
(a) Ideal vertical folded dipole, freespace.
(b) Practical vertical folded dipole, freespace.

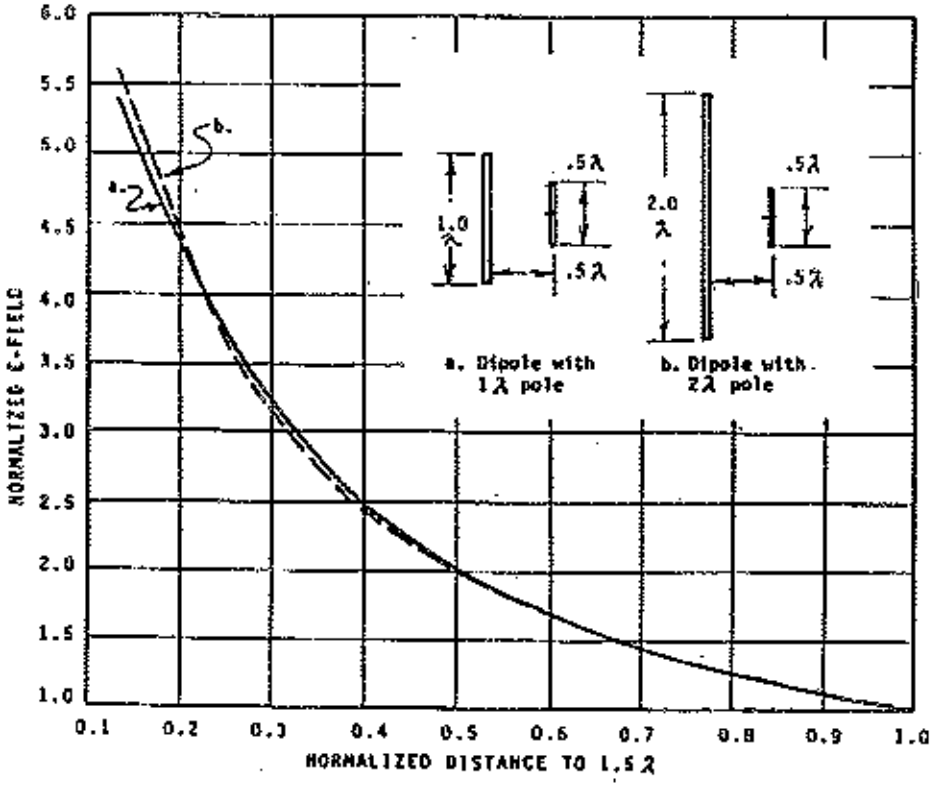

Figure 3-4. Correction factor vs normalized distance
(a) Folded vertical dipole near 1λ metal pole.
(b) Folded vertical dipole near 2λ metal pole.

Near-Field Intensity Curves and Normalization Distance for the Corner Reflector Antenna

The section on the corner reflector antenna (p. 3-24) points out the intermediate characteristics of this radiator between wire and aperture antennas. Numerical computations with NEC-BSC show that when the field intensity is normalized to distances greater than or equal to 5λ, it is nearly independent of aperture size within the popular design range of $1.5\lambda^2$ to $20\lambda^2$. Therefore, 5λ was chosen as the normalization distance.

Corner reflector correction curves behave like the wire curves discussed earlier. This similarity was also seen in the NEC-BSC runs, wherein the near-field E-vector was predominantly colinear with the radiator (typically a thin halfwave or bowtie element).

Derivation of Near-Field Calculations

An algorithm will now be outlined for calculating the on-axis near-field power intensity for three classes of antennas: wire, aperture, and corner reflector. In all cases, the far-field power intensity at the normalized distance (d) is multiplied by a correction factor taken from the correction curve for a particular antenna type (e.g., Figure 3-3 for a folded dipole).

The E-field intensity is used for all calculations in this report because it yields a higher, and therefore, more conservative correction than the H-field intensity in all the antennas under consideration, including the corner reflector, an aperture antenna. Generally, the magnetic field strength is included in near-field exposure studies.

Initially, the normalized distance corresponding to the actual distance considered is found by the proportional relationship:

$$d_W = R/(1.5\lambda) \qquad \text{[WIRE ANTENNAS ONLY]} \qquad (3\text{-}1)$$

where: d_W = normalized distance for wire antennas

R = distance under consideration, in meters

λ = wavelength, in meters

Similarly,

$$d_A = R\lambda/(2D^2) \qquad \text{[APERTURE ANTENNAS ONLY]} \qquad (3\text{-}2)$$

where: d_A = normalized distance for aperture antennas, in meters

D = largest aperture length, in meters

Similarly,

$$d_C = R/(5.0\lambda) \quad \text{[CORNER REFLECTORS ONLY]} \tag{3-3}$$

where: d_C = normalized distance for corner reflectors

The derivations of the near-field power equations for wire, aperture, and corner reflector classes follow. Input values are wavelength, mainlobe on-axis distance from the antenna, power input to the antenna, and power referenced to an isotropic source.

The far-field power for any antenna is

$$P_F = p_t g_t / (4\pi R^2) \tag{3-4}$$

where: P_F = far-field power density, in watts/m^2

p_t = antenna input power, in watts

g_t = antenna gain referenced to an isotropic source (gain in dBi must be converted to a power ratio)

The near-field and far-field intensities are related by

$$E_N = E_F (CF)_E \tag{3-5}$$

where: E_N = near-field E intensity, in volts/meter

E_F = far-field E intensity, in volts/meter

$(CF)_E$ = E-field correction factor at d

By definition,

$$P_F = (E_F)^2/(120\pi) \tag{3-6}$$

where: 120π = intrinsic free-space impedance, in ohms

Assuming: $P_N = (E_N)^2/(120\pi)$

where: P_N = near-field power density, in mW/cm^2

Combining Equations 3-4, 3-5, and 3-6,

$$P_N = .00796\ p_t\ g_t\ [(CF)_E/R]^2 \qquad (3\text{-}7)$$

From Equation 3-1, for wire or linear antennas,

$$R = 1.5\lambda \qquad (3\text{-}8)$$

Combining Equations 3-7 and 3-8,

$$P_N = .00354\ p_t\ g_t\ [(CF)_E/\lambda]^2 \qquad \text{[WIRE ANTENNAS]} \qquad (3\text{-}9)$$

From Equation 3-2, for aperture antennas,

$$R = 2\ D^2/\lambda \qquad (3\text{-}10)$$

Combining Equations 3-7 with 3-10,

$$P_N = .00199\ p_t\ g_t\ [(CF)_E\ \lambda/D^2]^2 \qquad \text{[APERTURE ANTENNAS]} \qquad (3\text{-}11)$$

From Equation 3-3, for corner reflectors,

$$R = 5.0\lambda \qquad (3\text{-}12)$$

Combining Equation 3-7 with Equation 3-11,

$$P_N = .000318\ p_t\ g_t\ [(CF)_E/\lambda\ ]^2 \qquad \text{[CORNER REFLECTOR]} \qquad (3\text{-}13)$$

The first eight of the nine antenna types selected for on-axis analysis, listed by group types on page 3-3, will use the wire Equations 3-1 and 3-9; whereas, the remaining corner reflector has its own Equations 3-3 and 3-13.

The aperture equations will not be used for on-axis analysis in this report. They are placed in this report in the event that correction coefficient curves generated from published data and numerical models are available. Examples of the former are the on-axis circular and rectangular aperture curves in Reference 2. For the latter, Section 4 provides procedures and examples of off-axis numerical modeling resulting in correction curves usable for the aperture equations.

Calculation Procedure: On-Axis Near-Field Power Intensity

In summary, the steps for calculating the near-field on-axis power density of an antenna type are as follows.

1. Select a normalized correction curve for a specific antenna type.
2. Calculate the normalized distance (d) by substituting wavelength and the distance under consideration (R) into Equation 3-1 for wire antennas, 3-2 for aperture antennas, or 3-3 for corner reflectors.
3. From the correction curve, find the correction factor $(CF)_E$ corresponding to d.
4. Calculate the near-field power density (P_N) at R from Equation 3-9 for wire antennas, 3-11 for aperture antennas, or 3-13 for corner reflectors using $(CF)_E$ and the specified input parameters.

FOLDED AND COAXIAL DIPOLE, SINGLE AND STACKED

General Considerations

One percent of government transmitting antennas employ the folded dipole, a design that falls well within the linear or wire antenna category according to the last two columns of TABLE 3-1. This is a widely used antenna in the VHF-UHF band for transmitting and receiving, and can be found by itself or as the single driven element in a multi-element antenna, e.g., in the conventional Yagi design discussed in Reference 2.

Single Folded Dipole

The ideal folded dipole is basically a halfwave antenna formed by shaping a loop into a thin rectangle as shown in the inset of Figure 3-3, where the width is less than a tenth of the halfwave length. At UHF, the smaller antenna dimensions make self-supporting lightweight tubular designs of low windload popular and practical (inset, Figure 3-3). Also, the fourfold increase in characteristic impedance and the retention of a balanced feedline make its implementation easier than for the thin-wire halfwave antenna from which it was derived. For a readable technical account of this common

antenna, consult Balanis,[15] which is based on a development from transmission line theory.[16]

Near-field calculations for 20-segment models of the ideal folded dipole antenna and the practical self-supporting one are plotted in Figure 3-3. As outlined previously, the field intensity and distance are normalized to a distance that is considered just within the far-field. Here, as for most wire antennas, it is 1.5 λ. The curve for the ideal folded dipole is seen to be nearly identical to that of the halfwave dipole on page 4-48 of Reference 2. Also, the practical antenna's intensity is always less than that of the ideal curve at distances greater than 0.133λ; therefore, the ideal curve is the choice for conservative radiation hazard calculations.

Calculation Procedure: - Single Folded Dipole

The foregoing suggests that the near-field of a vertical folded dipole in free-space may be found by following the four-step calculation procedure on page 3-12 of this report. First, calculate the normalized distance (d) from Equation 3-1, then find the correction factor from the ideal antenna curve [Figure 3-3a]. Finally substitute this factor into Equation 3-8 along with other input values, to get the power intensity. By using the ideal dipole curve whose correction values are always higher than the practical one, the estimates will be on the conservative side.

Example: Given the following input quantities, determine the power density at 1.2 m:

Frequency = 150 MHz (λ = 2.0 m)

Antenna power p_t = 100 watts

Antenna gain g_t = 2.1 dBi (1.62 power ratio)

Substituting λ and distance into Equation 3-1:

$$d_W = 1.2 / (1.5(2.0)) = 0.4$$

From Figure 3-3a, the normalized distance 0.4 corresponds to a correction factor $(CF)_E = 2.5$.

Substitute g_t, p_t, $(CF)_E$, and λ into Equation 3-9:

$$P_N = .00354\ (100)(1.62)(2.5/2.0)^2$$

$$= .0896\ mW/cm^2 \text{ at } 1.2 \text{ m distance}$$

---

[15] Balanis, C.A., *Antenna Theory, Analysis and Design*, pages 340-346, Harper and Row, Inc., New York, NY, 1982.

[16] Thiele, G.A., E.P. Ekelman, and L.W. Henderson, *On the Accuracy of the Transmission Line Model for Folded Dipole*, IEEE Transactions Antennas and Propagation, vol. AP-28, No. 5, pp. 700-703, September 1980.

Stacked Folded Dipole Array

For high power VHF-UHF transmission, a popular design employs folded dipoles equally spaced along a vertical supporting pole. Tilston reports that for noninteracting dipoles, changing the alternate arrangement of dipoles to an offset one simply translates an omnidirectional radiation pattern 6 dB in the direction of the offset.[17] Tilston shows that decreasing the latter's dipole offset to one half wavelength from the supporting mast will produce an elliptical pattern with a 6 dB gain. Apparently for this type of pattern, there can be little deviation from the omnidirectional pattern of a single folded-dipole; hence, the best attainable gain is an additional 6 dB.

The previous paragraph implies that the supporting pole has little effect on the nearby dipole. This supposition was tested and affirmed with a numerical model of dipoles spaced half a wavelength from supports one and two wavelengths long (inset, Figure 3-4). Except for the predicted antenna gain, the plotted results (Figure 3-4) are nearly identical to the situation where no poles are present (Figure 3-3).

The foregoing discussion, based on MININEC calculations, agree with a recent numerical and measurement analysis of practical folded dipole antennas mounted on metallic masts by Kahlor and Mallahzadeh.[18] Their analysis revealed that the effect of the mast itself enters primarily at subresonance length (see Figures 3 and 4 in Reference 18) and is therefore, negligible.

Calculation Procedure: Stacked Folded Dipole Array

The stacked folded dipole array and the single folded dipole in freespace are similar in near-field characteristics except for antenna gain. Consequently, the procedure for calculating the near-field of the folded dipole, including the correction factor for the freespace folded dipole (Figure 3-3, curve a), also applies to the stacked folded dipole array. The antenna gain will vary from about 1.6 (2.1 dBi) for a single dipole to a maximum of 6.4 (8.1 dBi). The latter figure can be derived from the definition:

$$P_s/P_i = (P_f/P_i)\,(P_s/P_f) \qquad (3\text{-}14)$$

where: P_s/P_i = stacked folded dipole array gain referenced to an isotropic antenna, in dBi

P_f/P_i = folded dipole antenna gain referenced to an isotropic antenna approx. 1.6 (2.0 dBi)

---

[17] Tilston, W.V., *On Evaluating the Performance of Communications Antennas*, IEEE Communications Magazine, pp. 700-703, September 1980.

[18] Kalhor, H.A. and A.R. Mallahzadeh, *Analysis of a Folded Dipole Antenna Mounted on a Cylindrical Metallic Mast*, IEEE Transactions on Antennas and propagation, volv. AP-34, no. 1, pp. 99-103, January 1986.

P_s/P_f = stacked folded dipole array gain referenced to a folded dipole antenna, max. 4.0 (6.0 dB)

Coaxial Dipole, Single, and Stacked

The coaxial dipole is a halfwave dipole with one half of the antenna inside a coaxial cable that also acts as the transmission line. Since the radiation pattern is similar to a halfwave dipole, the near-field correction is the same as for the folded dipole antenna (Figure 3-3, curve a). The stacked array radiation charactistics would also apply for widely separated non-interacting dipoles.

Calculation Procedures: Coaxial Dipoles, Single, and Stacked

The procedure outlined in this section for the folded dipole, single and stacked, also applies to the coaxial dipole because their radiating characteristics are identical.

OMNIDIRECTIONAL ANTENNAS - STUB TO DISCONE

General Considerations for Omnidirectional Antennas

Although omnidirectional antennas are listed separately in the GMF (TABLE 3-1), in reality, other antenna types are omnidirectional and can be placed in this category. These are the stub, ground-plane, coaxial, and discone antennas (Figure 3-5 to 3-7). A few facts about these emitters may be gleaned from TABLE 3-1.

1. Their total number is 12,136 and they comprise 12% of the total number of antennas in TABLE 3-1.

2. They are generally low-frequency low-gain linear radiators with the exception of 13% of the stub antennas that are at 1.2 GHz or higher.

As the name implies, a radially symmetrical signal is broadcasted from an antenna vertical to a conducting flat or sloping groundplane. The radiating element varies in configuration from the narrowband quarterwave whip of a groundplane aerial to the broadband cone of a discone antenna. The groundplane - always a good conductor-ranges from stiff radial wires to sheet metal discs and cones.

MININEC near-field intensities were plotted for all omnidirectional types and compared against more elementary basic antenna correction curves. With the exception of discones, the vertical E-field vector was two orders of magnitude greater than in the horizontal direction. The analysis and calculation procedures for each type of omindirectional antenna follow.

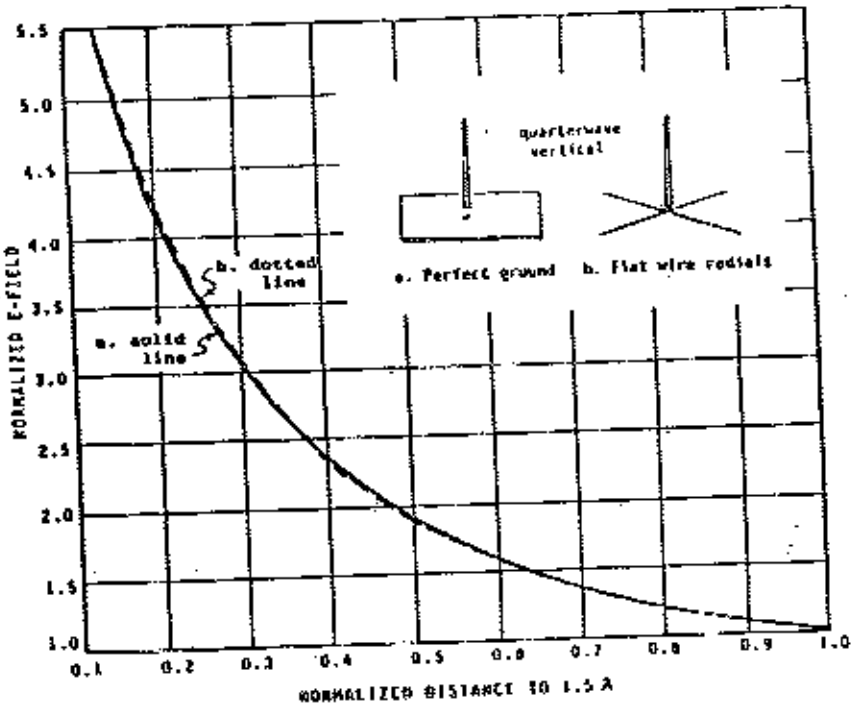

Figure 3-5. Correction factor vs normalized distance
(a) Groundplane antenna, flat perfect ground
(b) Groundplane antenna, flat wire radials

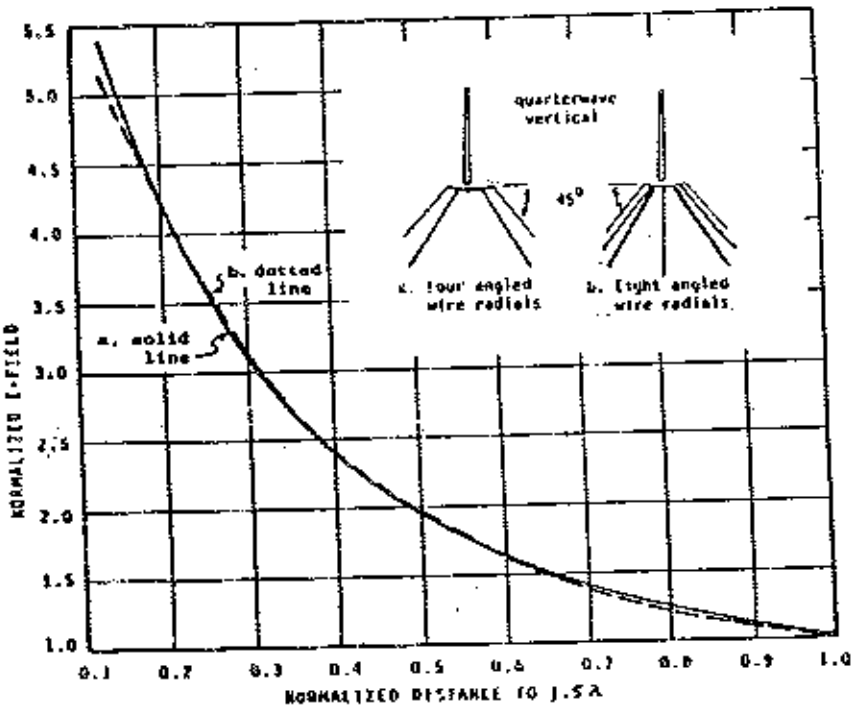

Figure 3-6. Correction factor vs normalized distance
(a) Groundplane antenna, four angled wire radials
(b) Groundplane antenna, eight angled wire radials

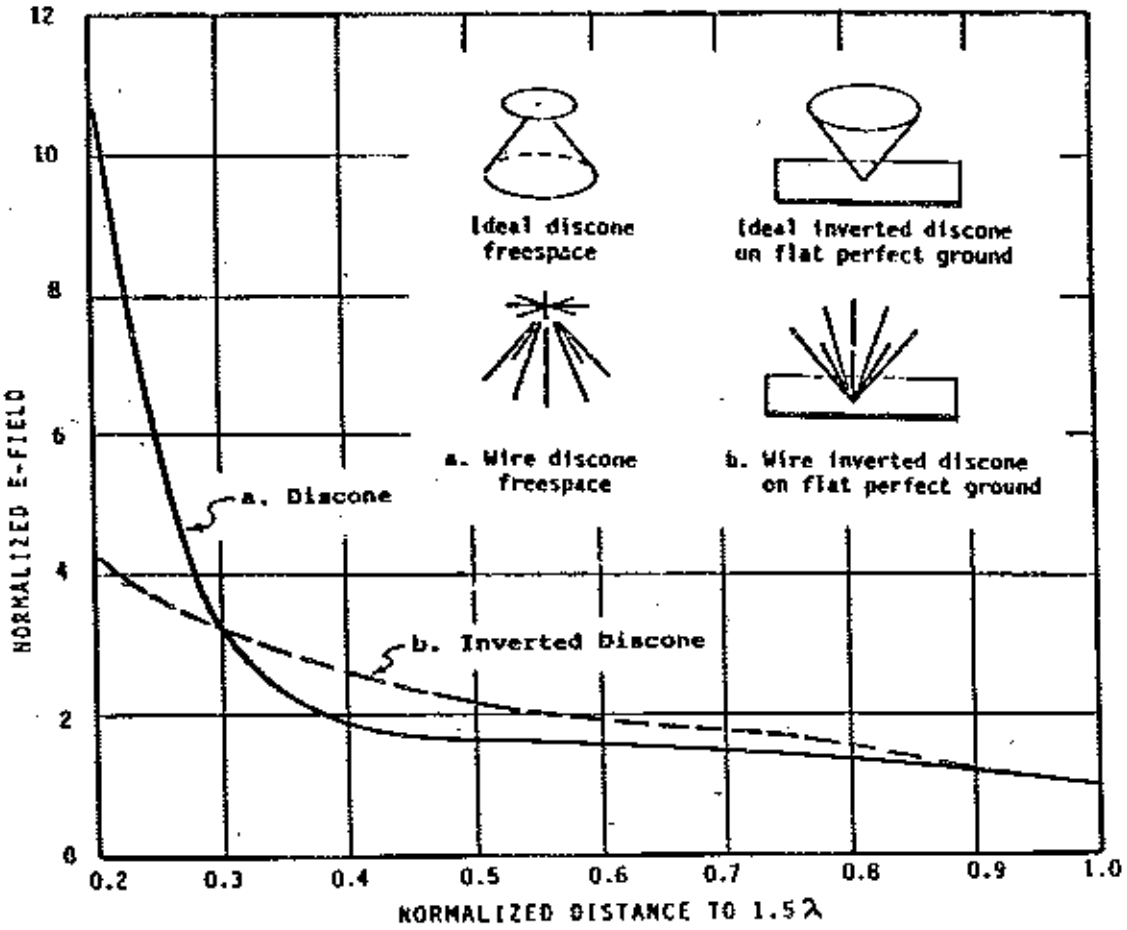

Figure 3-7. Correction factor vs normalized distance
(a) Discone, wire type, freespace
(b) Inverted discone, wire type, flat perfect ground

Stub and Blade Antennas

Most stub antennas and their streamlined counterparts called blade antennas are found as a self-supporting VHF-UHF quarter-wave radiators using an aircraft's metal surface as a ground plane. The leading edges of the empennage are favored sites because coverage can then be greater than a hemisphere. However, careful placement on the top or bottom centerline of the fuselage can also produce good hemispheric omnidirectional patterns.[19]

For the stub or blade, numerical calculations of a basic base-loaded quarter-wave vertical wire model above a perfectly conducting plane would lead to conservative radiation hazard estimates. MININEC data for such a model is plotted as a correction curve in Figure 3-5a.

Calculation Procedure - Stub and Blade Antennas

The stub calculation procedure below is valid as close as a tenth wavelength from the antenna, but does not account for the presence of conducting surfaces other than a ground plane. The effect of flaps and landing gear may be considerable (see Reference 19, p. 37-26); if so, appropriate numerical EM codes such as NEC-BSC (Section 4) may be necessary to model aircraft surfaces.

To calculate the near-field of stub and blade antennas over a flat conducting surface, consult the procedure outlined for wire antennas on page 3-11 of this report, and the correction curve for a basic quarterwave antenna (Figure 3-5a).

EXAMPLE: Given the following input quantities, determine the power density at 0.2m:

Frequency = 300 MHz (λ = 1.0 m)

Antenna gain g_t = 3 dBi (2.0 power ratio)

Antenna power p_t = 150 Watts

Substitute distance and in Equation 3-1:

$$d_W = 0.2/[1.5(1.0)] = 0.133$$

From Figure 3-5a, the normalized distance 0.133 corresponds to a correction factor $(CF)_E$ of 5.5.

---

[19] Johnson, R.C. and H. Jasik, *Antenna Engineering Handbook*, pp. 37-26, 37-27, McGraw-Hill Book Co., New York, N.Y. 1961.

Substitute g_t, p_t, $(CF)_E$, and λ into equation 3-9:

$$P_N = .00354\ (150)(2.0)(5.5/1.0)^2$$

$$= 32.13 \text{ mW/sq-cm at 0.2 m distance}$$

Ground-plane Antenna

A conducting flat surface or its equivalent is essential to the definition of the ground-plane antenna. There are over 5000 antennas in this category comprising 6% of the antennas in TABLE 3-1. They fall well within the wire antenna group according to the table. The basic configuration for groundplane antennas is the vertical halfwave dipole with the lower half replaced by a conducting plane termed the groundplane (Figure 3-5a). In practice, many variations can be discerned (Figures 3-5b and 3-6).

Theoretically a large, perfectly conducting ground plane will reflect all the radiation from the quarterwavelength wire, thus doubling total radiated power to yield a 3 dB gain over a halfwave dipole.[20] This gain is seldom achieved in practice, but can serve as an upper bound on the capability of this antenna type. The ground plane itself varies from radial wires, which are cantilevered on a supporting mast or embedded in the ground at MF to UHF, to flat metal plates at UHF and SHF. The ground-plane is often angled at about 45% (inset, Figure 3-6) to offset a raised mainlobe pattern sometimes encountered at VHF and UHF.

MININEC normalized E-field curves were generated for the three common ground-plane antennas (Figures 3-5b and 3-6). These curves compare closely to curve a, Figure 3-5, for normalized distances greater than 0.15. Thus the quarterwave vertical antenna over a perfect ground furnishes a useful correction curve for the ground-plane thin-vertical omnidirectional antennas.

Calculation Procedure - Ground-plane Antenna

The ground-plane calculation procedure is the same as for the stub antenna (p. 3-18), the first type described in this section on omnidirectional antennas. According to the MININEC calculations, the normalized distance should be at least 0.15. The correction curve to be consulted is the one for the quarterwave vertical over a perfectly conducting ground (Figure 3-5a).

Discone and Inverted Discone

The discone developed from the biconical dipole nearly fifty years ago by replacing a quarter-wave section with a conducting disc or a groundplane (Figure 3-7). This antenna type comprises 3% of the Federal transmitting antennas listed in the GMF (TABLE 3-1).

---

[20] Jessop, G.R., *VHF/UHF Manual, Fourth Edition*, p. 8.32, Radio Society of Great Britain, Hertfordshire, England 1983.

Segmented radial construction and a simple antenna feed are features it shares with its close relative, the groundplane antenna. However, the discone's outstanding characteristic is the ability to cover several octaves in frequency with little change in input impedance or the omnidirectional radiation pattern.[21] Initially applied at VHF-UHF (pages 70W and 71W of Reference 21), its relative ease of construction and maintenance as a large wire structure saw early adaptation at lower frequencies. One HF design requires no tuning or matching networks over a 3-to-1 frequency range.[22]

When a disc is not practical or desirable, the radiating cone can be inverted and placed over ground radials. An example of this inverted discone design in Figure 3-7b extends the range of wire discones into the LF band where an elevated wire disc would be difficult to construct (page 25 of Reference 22). In common with the groundplane antenna, a higher radiation angle results from having the antenna fed close to ground.

The near-field intensity of the discone and inverted discone numerical models (Figure 3-7) is greater than those of the basic quarterwave vertical over a conducting plane (Figure 3-5a) at near-antenna normalized distances. Therefore, for these types of broadband omindirectional antennas special curves are needed. Since the non-inverted discone yields the higher intensity at distances up to 0.3 λ from the antenna, it is the choice for the correction curve of discone antennas.

Calculation Procedure - Discone and Inverted Discone

The near-field of a discone or inverted discone may be assessed for radiation hazard by following the four-step procedure on page 3-11 of this report. The non-inverted discone correction curve is used at normalized distances equal to, and greater than 0.2. This correction curve (Figure 3-7a) should be used for frequencies well within the operating band of the discone.

The broadband characteristics of the discone (or any broadband antenna) makes the radiation pattern somewhat frequency dependent at the band edges. At the upper end of the band, the far-field single lobe which emanates at a low elevation angle is replaced by two or more shallow lobes (pages 65-68 of Reference 22; Reference 19, pages 4-15 and 26-15). The angles of these lobes and their relative gain with respect to the mainlobe at the lower cutoff frequency need to be considered when working at the band edges. The lower cutoff frequency is determined by the electrical length of the slope of the radiating cone.

---

[21] Kandoian, A.G., *Three New Antenna Types and Their Applications*, Procedures IRE (IEEE), vol. 34, pp. 70W-75W, February 1946.

[22] Collins Radio Company, *Collins High-Frequency Antennas/Selection/Applications* p. 24, Research Division, Collins Radio Co., Cedar Rapids, Iowa, May 1, 1961.

Example: Given the following input quantities, determine power density at 0.3 m:

Frequency = 300 MIIz (λ = 1.0 m)

Antenna gain g_t = 2.1 dBi (1.6 power ratio)

Antenna power p_t = 100 watts

Substitute distance and λ in Equation 3-1:

$$d_W = 0.3 /[1.5(1.0)] = 0.2$$

From Figure 3-7a, the normalized distance 0.2 corresponds to a correction factor $(CF)_E$ of 11.0.

Substitute g_t, p_t, $(CF)_E$, and λ into Equation 3-9:

$$P_N = .00354\ (100)(1.6)(11.0/1.0)^2$$

$$= 68.53 \text{ mW/sq-cm at 0.3 m distance}$$

DIPOLE AND STACKED ARRAYS

General Considerations

Dipole and stacked arrays make up 3% and 1% respectively of all Federal transmitting antennas (TABLE 3-1). Since stacked arrays usually consist of dipoles arranged vertically, they fall within the category of "dipole arrays" and will not be considered as a separate antenna type. In this part of the report, uniformly-spaced halfwave dipoles are assumed, which interact in a linear array to radiate a bilaterally symmetrical azimuthal pattern. Stacked arrays with dipoles spaced far enough to be non-interacting were covered on pages 3-13 and 3-14.

Differential phase and magnitude of excitation at antenna inputs and variable antenna spacing will give rise to an infinite number of radiation patterns. But for the same excitation vector applied to each element of a uniformly spaced array, the broadside and endfire designs concentrate radiation best in the main lobes. Therefore, they are selected for radiation hazard assessment, their configurations defined, and procedures outlined for calculating near-field on-axis power intensities.

Broadside Dipole Array

If the dipoles in a linear array are spaced a halfwave apart and fed in phase, a far-field broadside radiation pattern will result with nulls along the array axis. This is seen in Figure 3-8 where the mainlobes are along the x-axis and the nulls on the y-axis. The near-field radiation has a similar pattern.

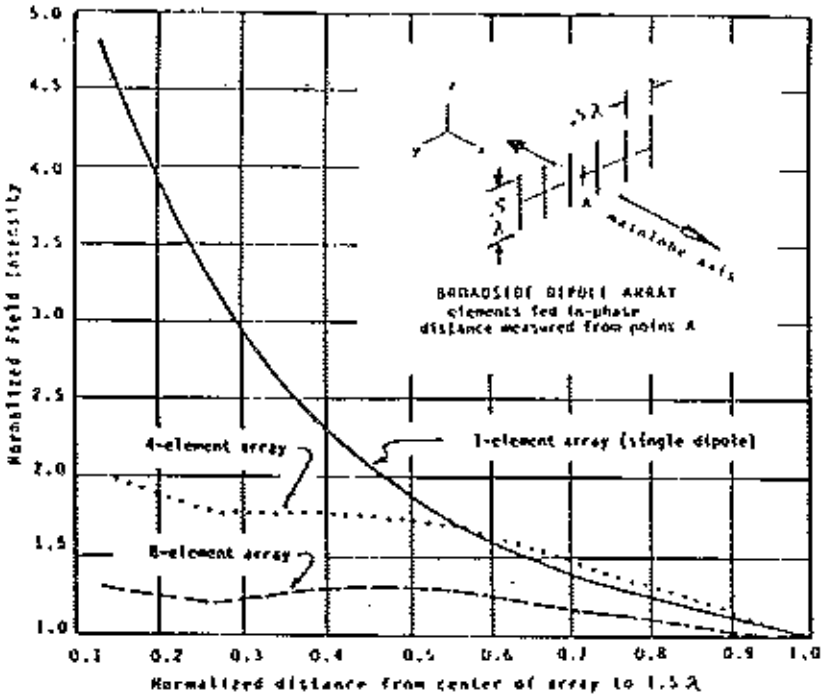

Figure 3-8. Correction factor vs normalized distance
(a) Halfwave verticle dipole, free space
(b) 4-element broadside vert. dipole array, freespace
(c) 8-element broadside vert. dipole array, freespace

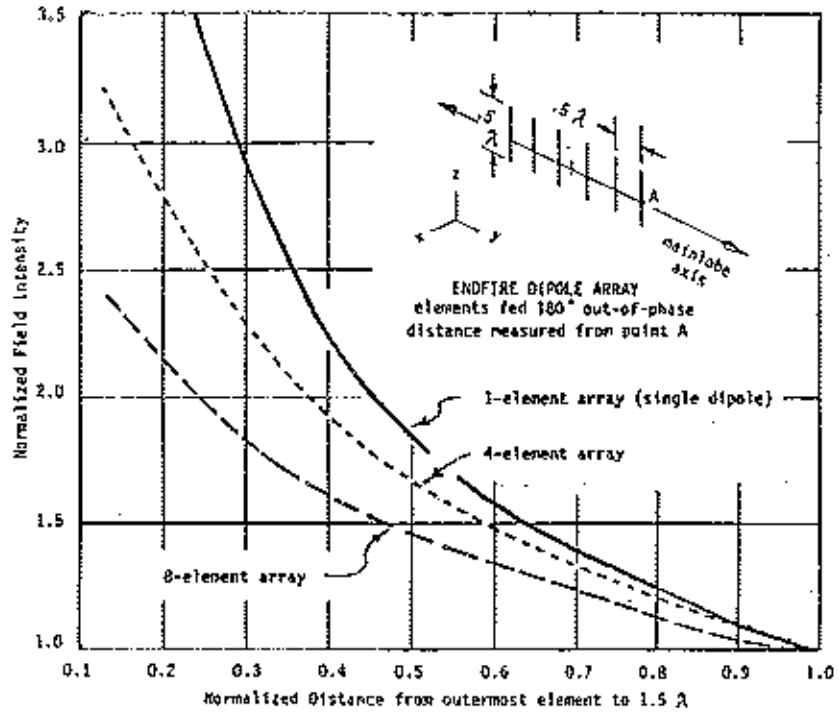

Figure 3-9. Correction factor vs normalized distance
(a) Half-wave vertical dipole, freespace
(b) 4-element endfire vert. dipole array, freespace
(c) 8-element endfire vert. dipole array, freespace

MININEC results for 1-, 4-, and 8-element arrays are plotted as normalized curves in Figure 3-8. Since the 1-element array (in reality a single halfwave dipole) has E-field intensities higher than the others at all distances, it becomes the conservative choice for the near-field correction of broadside dipole arrays.

Calculation Procedure - Broadside Dipole Array

To calculate the near-field on-axis power intensity of a broadside linear dipole array in freespace, follow the procedure outlined on page 3-12 of this report. The correction curve for the 1-element array (halfwave dipole) at normalized distances exceeding 0.15 should be employed for conservative results.

EXAMPLE: Given the following for a multi-element broadside dipole array, find the power density at 0.2 m:

Frequency = 600 MHz (λ = 0.5 m)

Antenna gain g_t = 20 dBi (100 power ratio)

Antenna power P_t = 20 Watts

Substitute distance and wavelength in Equation 3-1:

$$dW = 0.2 /[1.5(.5)] = 0.266$$

From Figure 3-8 the normalized distance 0.266 corresponds to a correction factor $(CF)_E$ of 3.2.

Substitute g_t, p_t, $(CF)_E$, and λ into Equation 3-9:

$$P_N = .00354\ (100)(20)(3.2/.5)^2$$

$$= 290\ \text{mW/sq-cm at 0.2 m distance}$$

Endfire Dipole Array

If the linear dipole arrays of Figure 3-8 (also with elements spaced halfwave apart) are excited with a phase shift of 180 degrees between adjacent elements, the endfire pattern of Figure 3-9 results with nulls in the x-direction. The elements themselves are now on the mainlobe axis and distance cannot be measured in the same manner as for the broadside array. By taking the midpoint of the outermost element of the array as the starting point, two advantages are gained:

1. The avoidance of an ambiguous correction factor when a distance chosen for analysis corresponding to the location of an element.

2. Distance can still be normalized to 1.5λ and be independent of location and number of elements.

MININEC endfire data for 4- and 8-element arrays normalized to 1.5λ from the outermost element are plotted in Figure 3-9. As with the broadside array, the 1-element array (vertical halfwave dipole) has higher correction factors than any of the endfire arrays. Therefore its correction factor curve will also apply to endfire arrays.

Calculation Procedure - Endfire Dipole Array

To calculate the near-field on-axis power intensity of an endfire dipole linear array in freespace, follow the procedure outlined for the broadside case on the previous page with the following important difference:

Distance is normalized to the midpoint of the outermost element in an array; therefore, the distance from the array's electrical center (also its geometrical center in a linear array) to the outermost element must be known. This can be found by the simple relationship:

$$D_E = (N-1)\,\lambda/4 \qquad (3\text{-}15)$$

where: D_E = distance from the electrical center to the outermost element in meters.

N = number of elements (dipoles) in the array.

λ = wavelength in meters.

CORNER REFLECTORS

General Considerations

Corner reflector antennas make up 3% of Federal Government RF radiators and fall into the wire (linear) category according to TABLE 3-1. This type of antenna consists of two parts, readily seen in Figures 3-10 and 3-11:

1. a metallic reflector consisting of two plane surfaces meeting at an included angle of 180 degrees or less, and

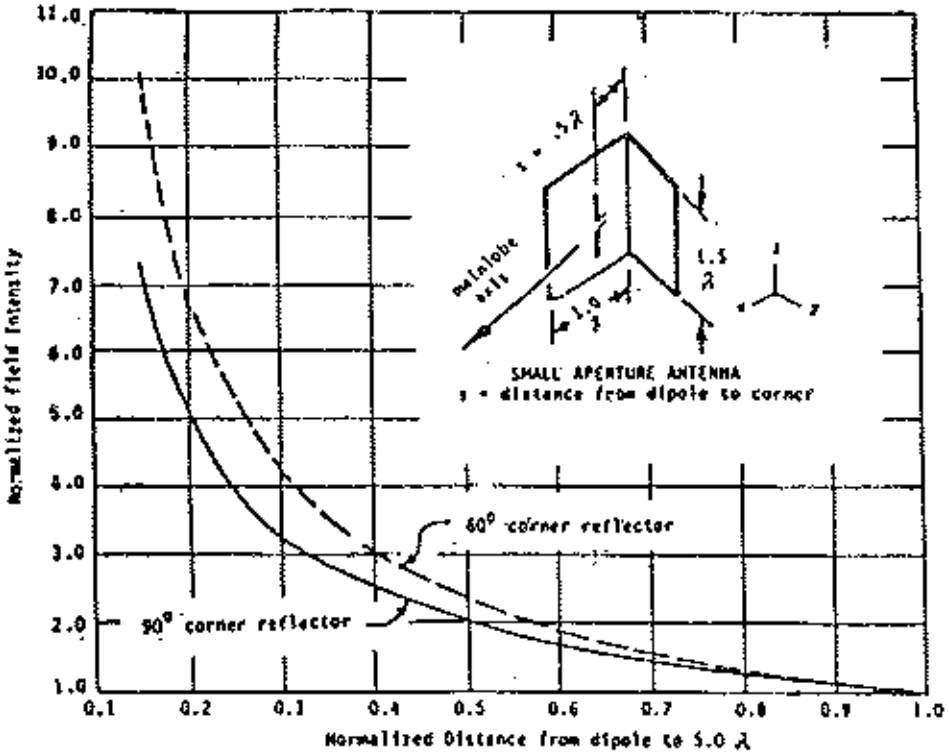

Figure 3-10. Correction factor vs normalized distance
(a) 90° small-aperture corner reflector, freespace
(b) 60° small-aperture corner reflector, freespace

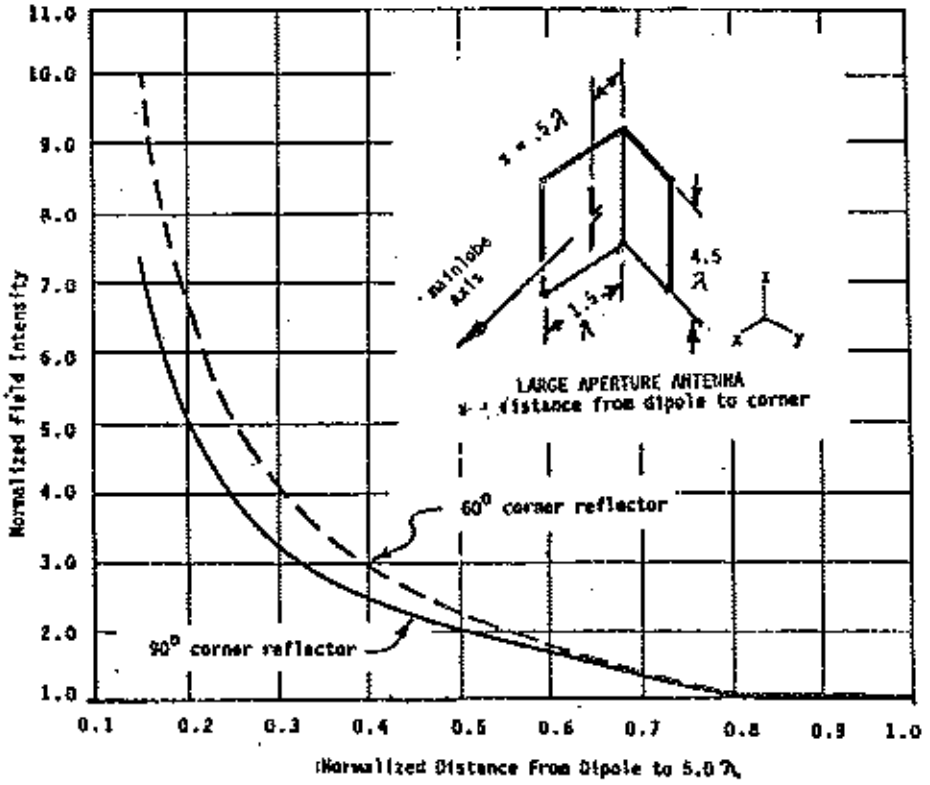

Figure 3-11. Correction factor vs normalized distance
(a) 90° large-aperture corner reflector, freespace
(b) 60° large-aperture corner reflector, freespace

2. a radiator, usually a thin-wire or bowtie halfwave dipole, placed equidistant to the plane surfaces.

Corner reflectors are like more expensive aperture antennas in that the reflector can increase forward gain by 12 dB or more with high aperture illumination.[23] Therefore, corner reflectors are often low-cost replacements for horns and dishes in UHF applications where portability, ease of installation, and good beam directivity are desired.

Theoretically, the corner reflector is amenable to geometric optics analysis employing the Method of Images provided the included angle Φ_{CR} of the corner is an integral submultiple of π, i.e.

$$\Phi_{CR} = \pi/n \qquad n = 1, 2, 3, 4, \ldots$$

In Wolff [Reference 23, pp. 299-312], analytical expressions developed by the image method are derived for arbitrary Φ_{CR} and dipole orientation. Wolff's results are in graphical form and useful for practical design of corner reflectors.

In practice, the aperture must be at least a few-to-several square wavelengths in area, a requirement which generally restricts these antennas to frequencies above 200 MHz. A survey shows that nearly all have a 60- or 90-degree reflector, an aperture area of at least 3 square-wavelengths, and a halfwave dipole (wire or bowtie) oriented parallel to the reflector's vertex (see Reference 15, pp. 594-597).

The vertex-to-dipole distance in wavelengths (termed "s") is a sensitive parameter in corner reflector design. For the 90-deg. reflector, the far-field radiation changes from a single- to a double-lobed pattern when s goes from 0.1 to 1.0λ (see Reference 15, p. 600). Corresponding lobes found in the near-field are probably due to the large θ (zenith angle) E-vector at near distances for a vertically oriented dipole (see Reference 7, Part 1, pp. 729-730). Reference 19 pp. 17-3 to 17-5 show far-field patterns for Φ_{CR} = 60, 120, and 180 degrees that have similar pattern changes as the 90-deg. reflector. In general, directivity and sidelobe suppression improves with a narrower corner angle and for s less than 0.7 λ. However, feed impedance drops rapidly under the same conditions, and impair antenna gain and impedance matching (see Reference 20, p. 8.23). A survey of corner reflector specifications by various manufacturers and radio societies showed that approximately 0.5 λ to be the most common s-parameter value.

NEC-BSC Calculations

Typical dimensions for 60- and 90-degree corner reflector models were inputted to the NEC-BSC, version 3, numerical code running on a MicroVAX-II computer (Figures 3-10 and 3-11). The NEC-BSC code based on the geometrical diffraction theory is more suitable for MININEC or NEC for surfaces with dimension about a

---

[23] Wolff, E.A., *Antenna Analysis*, page 302, J. Wiley & Sons, New York, N.Y. 1966.

wavelength or more typical of aperture antennas (cf Section 4). The calculated field intensities plotted from the VAX output (Figures 3-10 and 3-11) are normalized to the on-axis distance of 5λ for reasons stated on page 3-9.

A typical large aperture will give rise to a correction curve with a slightly higher intensity than for a smaller one. Since the two apertures of page 3-25 are the extremes of practical corner reflector size for a single dipole, the larger aperture (Figure 3-11) is chosen for conservative radiation hazard assessment.

Calculation Procedure - 60- and 90-Degree Corner Reflectors

To calculate the near-field on-axis power intensity of a 60-or 90-degree corner reflector, use Equations 3-3 and 3-13, and a large-aperture correction curve from Figure 3-11.

EXAMPLE: Given the following for a 90-deg. corner reflector find the power density at 0.1 m from the dipole.

Frequency = 3 GHz (λ = 0.1 m)

Antenna gain g_t = 14.0 dBi (25.1 power ratio)

Antenna input power p_t = 15.0 watts

Substitute R = 0.1 and λ into Equation 3-3:

$$d_C = 0.1 / [5.0(0.1)] = 0.20$$

From Figure 3-11, the normalized distance 0.20 corresponds to a correction factor $(CF)_E$ of 5.05 for the 90-degree large-aperture antenna.

Substitute p_t, g_t, λ, and $(CF)_E$ into Equation 3-13:

$$P_N = .000318\ (15.0)(25.1)(5.05/0.1)^2$$

= 305 mW/sq-cm at 0.1 m from the dipole

SUMMARY AND INCORPORATION INTO PC DISK

Summary of Additional Antennas for On-Axis Analysis

The updated GMF was culled for additional antennas not covered in this report's predecessor [Ref. 2]. Nine were selected for on-axis near-field analysis and placed in five basic categories. Simple procedures were developed for calculating power intensities from correction curves derived from numerical computation models. The basic categories and their antennas are:

1.	Vertical half-wave dipole:	Folded dipole Coaxial (dipole)
2.	Vert. quart.-wave at ground plane:	Stub (blade) Ground plane Omnidirectional
3.	Broadband omnidirectional:	Discone
4.	Linear arrays of dipoles:	Dipole array Stacked array
5.	Dipole with plane reflectors:	Corner reflector

The corner reflector is the only one analyzed as an aperture antenna rather than a wire antenna.

TABLE 3-2 lists the antennas and pertinent equations and correction curves for convenient reference. Before attempting calculations, the reader is strongly advised to read the detailed description of each antenna and to work through the accompanying example. An antenna may require a different interpretation even if it uses the same correction curve. For instance, compare the endfire and broadside dipole arrays on pages 3-20 to 3-22.

As an aid to antenna type selection, each of the 100,000 antennas in the GMF as shown in TABLE 3-1 was placed in two categories: frequency less or greater than 1.2 GHz and antenna gain less or greater than 18 dBi. Together with the earlier Procedures (Farrar and Chang 1987), this technical memorandum covers nearly 97% of the transmitting antennas in TABLE 3-1.

Incorporation of the Procedures into the AFI PC Program

The Antenna Field Intensity Program, AFI, is a PC-disk version of the calculation procedures in Reference 2. AFI works in demand-mode execution by prompting the user to input such parameters as antenna type and frequency. The correction factor needed to convert far-field intensity to near-field power is automatically calculated by one of two methods. The first finds the near-field power (for wire antennas) by a similar procedure to the one on page 3-11 of this report. The second method (for aperture antennas) integrates an aperture distribution function obtained from far-field input parameters to calculate a near-field correction.

TABLE 3-2

SUMMARY TABLE FOR ON-AXIS NEAR-FIELD POWER DENSITY CALCULATIONS*

Antenna Type from Table 3-I		Equations for Calculations Assuming $P_N = (E_N)^2/(120\pi)$	Correction factor $(CF)_E$
Blade		3-1, 3-9	Fig. 3-4a
Coaxial(dipole)		3-1, 3-9	Fig. 3-3a
Corner reflector		3-3, 3-13	Figs. 3-10a,b
Dipole array:			
	Broadside	3-1, 3-9	Fig. 3-7a
	Endfire	3-1, 3-9, 3-11	Fig. 3-7a
Discone:			
	with cap	3-1, 3-9	Fig. 32-6a
	Inverted	3-1, 3-9	Fig. 3-6a
Folded dipole		3-1, 3-9	Fig. 3-3a
Ground plane		3-1, 3-9	Fig. 3-4a
Omnidirectional		3-1, 3-9	Fig. 3-4a
Stacked array:			
	Folded dipole	3-1, 3-9, 3-10	Fig. 3-2a
	Coaxial	3-1, 3-9, 3-10	Fig. 3-2a
Stub		3-1, 3-9	Fig. 3-4a

*This table is for easy reference only. Before attempting calculations, the reader is strongly advised to read the detailed description of each antenna and to work through the accompanying example.

The AFI user has no need to consult correction curves or to substitute input parameters into algebraic expressions. At any point in program execution, the user is advised if the inputs entered thus far cannot be processed or could produce questionable data.

Incorporation of the nine antenna types discussed on the previous page to AFI's eight is accomplished through six lookup correction tables corresponding to the curves in Figures 3-3, 3-5, 3-7, 3-8, and 3-11.

Although the corner reflector resembles an aperture antenna, its near-field characteristics are more like a wire radiator. Therefore, simple wire-type lookup tables replace complex mathematical algorithms normally employed for aperture antenna calculations as exemplified by the aperture computations in the original AFI program.

SECTION 4

PROCEDURES FOR OBTAINING OFF-AXIS NEAR-FIELD INTENSITIES WITH NUMERICAL ELECTROMAGNETIC CODES

GENERAL CONSIDERATIONS

Introduction

The calculation of power density along the mainlobe axis of an antenna is a one-dimensional problem and fairly easy to interpret. But off-axis analysis is two or three dimensional and is extremely complex, particularly in the near field where E and H vectors are usually not orthogonal (*cf* Section 3). Taking the spherical coordinate system as an example, the radius vector r is joined by the azimuth angle Φ in the horizontal plane, and the zenith angle θ in the vertical plane.

The spatial description of power density is especially difficult in situations where the aperture distribution must be deduced from far-field characteristics. This is the case for on-axis analysis considered so far in this report and by its antecedent. The aperture algorithms (Reference 2, Section 4) apply only to on-axis analysis (Reference 2, p. 4-9) and not to two or three dimensions.

The Numerical Approach

Numerical methods of solving EM problems in experimentation and system installation are equally adaptable to radiation hazard assessment.[24] Accurate models and their algorithms, made practical by the advent of high-speed large-memory computers, and verification by automated measurements, have found wide application in antenna field analysis.[25]

Easy-to-use numerical codes that evaluate the near-field of radiators and their EM environment are available for the nonspecialist in interactive and non-interactive input modes. MININEC is an example of the former and NEC-BSC the latter. But if a formal presentation of numerical modeling is made, the following engineering practices should be followed:

1. Independent verification of the results, at least partially, should be done in some manner acceptable to peers. For example, comparisons could be made

---

[24] Kobayashi, H.K., *Modeling a Receiving MF-HF Phased Antenna Array: Numerical Computation vs Field Measurements*, Proceedings IEEE Region 1 Workshop on Electromagnetic Field Computation, Schenectady, NY, Volume II, pp. E-30 - E-34, October 20-21, 1986.

[25] Ryan, Jr, C.E., et al, *IEEE Transactions on Electromagnetic Compatibility*, vol. EMC-22, no. 4, pp. 244-255, November 1980.

with field and laboratory measurements, results from the usage of other numerical codes and computers, or from predictions based on statistical and mathematical models.

2. Repeatability of the results by an impartial observer. Sufficient data on the geometry of the model and other input parameters should be provided so that anyone can repeat the analysis with identical or similar numerical codes and computers.

Numerical Codes for Wire Antennas

The discussion in Section 3 on the on-axis usage of MININEC and NEC and in Ref. 2, pp. 4-5 and 4-9 applies equally well to off-axis wire antenna analysis. The following points should be considered in deciding whether an antenna is amenable to analysis with a thin-wire method-of-moment numerical code, such as the standard version of NEC-3, obtainable from its custodian, the Lawrence Livermore Laboratory.

1. The antenna and it electromagnetic environment (excluding ground) can be represented by thin-wires or small polygons.

2. Ground, whether perfect or imperfect, interact closely with antennas and must be accounted for.

3. Wire segments, each usually less than 0.1 λ in length, can be kept to a few hundred in number in order to limit CPU time.

Numerical Codes for Aperture Antennas

Ohio State University's Basic Scattering Codes discussed in Section 3 (also see Reference 2 pp. 4-4 and 4-5) are representatives of the Geometrical Theory of Diffraction (GTD) approach to solving antenna problems.

In many ways GTD codes complement the wire ones because large conducting and dielectric shapes to complicated to be modeled as wires can be easily represented. However, the smallest dimension is in the order of a wavelength (Reference 12, p. 239; Reference p. 1-2); thus limiting most applications to VHF and above. Fortunately the majority of aperture antennas operate well above the VHF band and pose little restriction on GTD analysis. For example, practical horn aperture dimensions are generally more than a few wavelengths in length.

The radiating elements may be difficult to specify for complicated aperture distributions and special input and output programs must be written for a code such as the NEC-BSC. An evaluation of the near-field radiation hazard of a large planar array was a typical modification of this type.[26,27] Koh replaced the aperture distribution formed by slot elements with simplified models (Figure 4-1). Computation time was reduced and the accuracy of the results was retained.

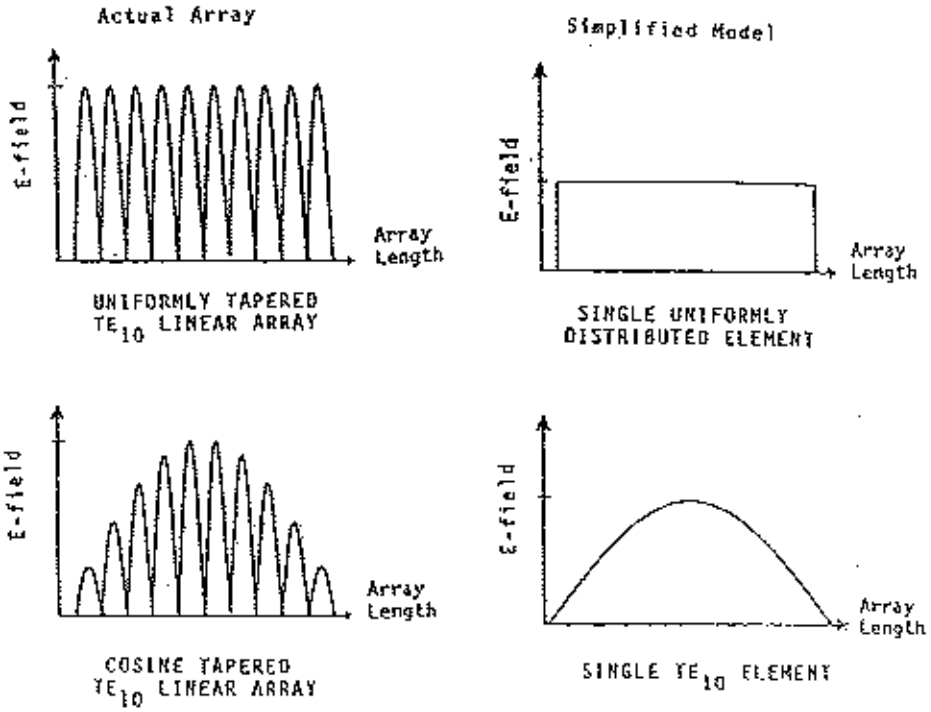

Figure 4-1. E-field distribution for a planar array, after Koh and Adler. (See Reference 27.)

---

[26] Koh, W.J., *Radiation Hazard Evaluation for a High Power Mobile Electromagnetic Radiation Weapon Using the Numerical Electromagnetic Code*, M.S. Thesis, Naval Postgraduate School, Monterey, CA, March 1987.

[27] Koh, W.J. and R.W. Adler, *Radiation Hazard Evaluation Using NEC-BSC*, Conference Proceedings 3rd Annual Review of Progress in Applied Computational Electromagnetics, Monterey, CA, March 24-26, 1987.

NEC-BSC is combined with the Aperture Integration (AI) method for analyzing parabolic reflectors in Ohio State University's NEC-REF program.[28] Despite certain limitations detailed in Reference 2, p. 4-5, NEC-REF should be seriously considered for radiation hazard analysis because:

1. NEC-REF appears to be as easily programmable as NEC-BSC, the code from which it was derived, and

2. the effect of feed blockage and scatter from feed struts can be included in near-field assessment.

GEMACS, A General Program For EM Field Analysis

The General Electromagnetic Model for the Analysis of Complex Systems (GEMACS) is the combination of the two physical approaches discussed so far: the Method-of-Moments (MOM) and the Geometrical Theory of Diffraction (GTD). In addition, the Finite Difference (FD) approach is included to analyze the interior of structures. Originally funded by the U.S. Air Force for EM compatibility analysis, GEMACS is ideally suited for radiation hazard analysis of antennas.[29]

The user defines the geometry and excitation of the antenna system and the outputs desired. The "hybridization methodology" (see Reference 29) coordinating the calculations done by one or more approaches is transparent to the user; however, by making GEMACS portable (i.e., usable to many DoD agencies) the preprocessing becomes tedious to enter and the postprocessing difficult to interpret. Rome Air Development Command is addressing this problem; meanwhile, GEMACS is available in FORTRAN for parties willing to use the code in its present form or to modify it.

The purposes of the rest of Section 4 are:

1. to present examples of off-axis analysis and verification of two different antennas by the numerical codes previously employed for on-axis analyses in Section 3, and

2. to outline the procedures by which the off-axis analyses were obtained from these relatively inexpensive, readily available, user-oriented codes.

---

[28] Rudduck, R.C. and Y.C. Chang, *Numerical Electromagnetic Code NEC-REF (Version 2) Part I: User's Manual*, The Ohio State U. ElectroScience Laboratory, Dept. of Electrical Engineering, Columbus, OH 43212, December 1982.

[29] Siarkiewicz, K.R., *GEMACS - An Executive Summary*, Applied Computational Electromagnetics Society (ACES) Newsletter, vol. 2, no. 1, pp. 124-136, May 1987.

MININEC ANALYSIS OF A BROADSIDE DIPOLE ARRAY

Introduction

This example of a near-field wire antenna analysis features the MININEC (Version 3) code on a IBM PC-AT desk computer. This is an off-axis power analysis of the 8-element broadside dipole array similar to the array in Figure 3-7, also in the horizontal x-y plane (inset, Figure 4-2). A wavelength of 1.0 m (300 MHz) was chosen for simplicity and ease in entering the antenna geometry and interpreting the output data. E-field intensity as a function of y was plotted for six near-field distances along the x-axis broadside to the array (Figure 4-2). All intensities were normalized to the highest value of the closest distance i.e. (x,y) = (0.2, 1.5). The curves then are applicable at all radio frequencies because spatial measurement is in units of wavelength as well as in meters.

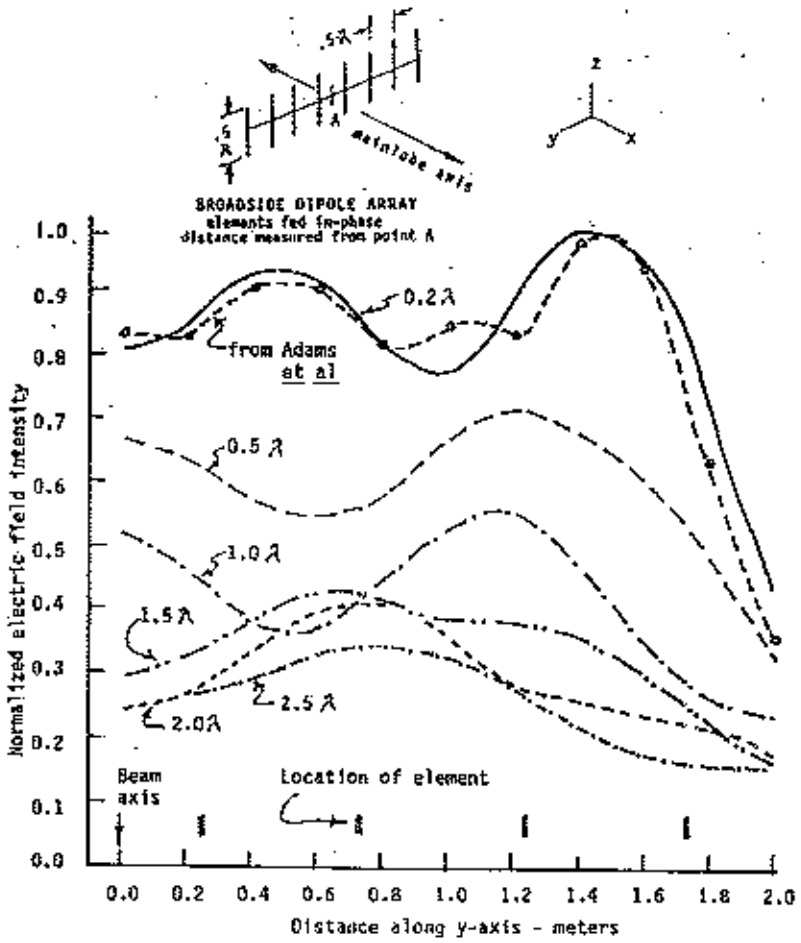

Figure 4-2. Off-axis near E-field intensity vs distance 8-element broadside vertical dipole array, freespace.

Analysis of Results

The curves show how intensity lessens and becomes more uniform across the face of the array when moving 0.2 to 2.5 λ in the x-direction away from the array's centerpoint. Data for a computer model of an identical array at x = 0.2λ (see Reference 5, Figure 6a) is plotted for comparison. Adams' code is similar to MININEC in utilizing the method-of-moment thin-wire approximation and pulse type expansion function (Reference 5, p. 262). The agreement is good even for the location of the maximum intensity at y = 1.5 m. Intensities at distances greater than 2.5λ (not shown) also compare in magnitude and shape.

Procedures for Implementing a MININEC model of a Broadside Dipole Array

The complete MININEC input data are listed on Table 4-1. Starting with frequency, the MININEC user is prompted to define the antenna's environment, geometry, and excitation. Each of the eight antenna elements is a halfwave six-segment thin wire. Elements are spaced halfwave apart in freespace and fed in-phase for broadside radiation. MININEC then takes two minutes to calculate and fill the wire-segment current matrix. Next, the far-field or near-field output is specified, and the power input may be changed if desired. Finally, calculations scroll on to the CRT screen as they are completed for each specified point in space. As options, input and output data can be stored in disk data files.

First-time users will find that basic MININEC code can be readily applied to thin-wire antennas (maximum 50 segments) in a simple environment. The latest version (3.0) has versatile input and output options too numerous to list here (see Reference 6). Also, there are special-purpose MININEC codes with features such as increased segmentation for certain antenna configurations.

Familiarization with MININEC (Version 3) starts with a mnemonic example in the user's guide (Reference 6, pp. 66-78). More help can be found in Reference 9, and the Annual Reviews of Progress and the Journal/Newsletter of the Applied Computational Electromagnetics Society (ACES) starting with 1984.

NEC-BSC ANALYSIS OF A 90° CORNER REFLECTOR

Introduction

This example of a near-field off-axis aperture antenna analysis features the NEC-BSC code on a MicroVAX-II computer. The antenna is the 90° corner reflector in Figure 3-11 with the critical corner-to-dipole distance s changed from 0.5λ to 1.18λ.

As stated earlier, NEC-BSC is based on the Geometrical Theory of Diffraction (Reference 12, pp. 238-242) and is not closely related NEC, the wire code. The corner reflector dimensions of Example 5 in Reference 7, Part 1, are used because experimental measurements are available for verification of our example.

TABLE 4-1

INPUT DATA FOR MININEC MODEL OF AN 8-ELEMENT DIPOLE ARRAY

```
OUTPUT TO CONSOLE, PRINTER, OR DISK (C/P/D)? C

FREQUENCY (MHZ)? 300

ENVIRONMENT (+1 FOR FREE SPACE, -1 FOR GROUND PLANE)? +1

NO. OF WIRES? 8

WIRE NO. 1
    NO. OF SEGMENTS: 6
    END ONE COORDINATES (X,Y,Z)? .25,0,.25
    END TWO COORDINATES (X,Y,Z)? .25,0,-.25
                        RADIUS? .005
WIRE NO. 2
    NO. OF SEGMENTS: 6
    END ONE COORDINATES (X,Y,Z)? -.25,0,.25
    END TWO COORDINATES (X,Y,Z)? -.25,0,-.25
                        RADIUS? .005
WIRE NO. 3
    NO. OF SEGMENTS: 6
    END ONE COORDINATES (X,Y,Z)? .75,0,.25
    END TWO COORDINATES (X,Y,Z)? .75,0,-.25
                        RADIUS? .005
WIRE NO. 4
    NO. OF SEGMENTS: 6
    END ONE COORDINATES (X,Y,Z)? -.75,0,.25
    END TWO COORDINATES (X,Y,Z)? -.75,0,-.25
                        RADIUS? .005
WIRE NO. 5
    NO. OF SEGMENTS: 6
    END ONE COORDINATES (X,Y,Z)? 1.25,0,.25
    END TWO COORDINATES (X,Y,Z)? 1.25,0,.25
                        RADIUS? .005
WIRE NO. 6
    NO. OF SEGMENTS: 6
    END ONE COORDINATES (X,Y,Z)? -1.25,0,.25
    END TWO COORDINATES (X,Y,Z)? -1.25,0,.25
                        RADIUS? .005
WIRE NO. 7
    NO. OF SEGMENTS: 6
    END ONE COORDINATES (X,Y,Z)? 1.75,0,.25
    END TWO COORDINATES (X,Y,Z)? 1.75,0,.25
                        RADIUS? .005
WIRE NO. 8
    NO. OF SEGMENTS: 6
    END ONE COORDINATES (X,Y,Z)? -1.75,0,.25
    END TWO COORDINATES (X,Y,Z)? -1.75,0,.25
                        RADIUS? .005
```

TABLE 4-1 CONTINUED

```
NO. OF SOURCES? 8

SOURCE NO. 1:
PULSE NO., VOLTAGE MAGNITUDE, PHASE (DEGREES)? 3,1,0

SOURCE NO. 2:
PULSE NO., VOLTAGE MAGNITUDE, PHASE (DEGREES)? 8,1,0

SOURCE NO. 3:
PULSE NO., VOLTAGE MAGNITUDE, PHASE (DEGREES)? 13,1,0

SOURCE NO. 4:
PULSE NO., VOLTAGE MAGNITUDE, PHASE (DEGREES)? 18,1,0

SOURCE NO. 5:
PULSE NO., VOLTAGE MAGNITUDE, PHASE (DEGREES)? 23,1,0

SOURCE NO. 6:
PULSE NO., VOLTAGE MAGNITUDE, PHASE (DEGREES)? 28,1,0

SOURCE NO. 7:
PULSE NO., VOLTAGE MAGNITUDE, PHASE (DEGREES)? 33,1,0

SOURCE NO. 8:
PULSE NO., VOLTAGE MAGNITUDE, PHASE (DEGREES)? 38,1,0

NUMBER OF LOADS? 0

********************** MININEC MENU ********************************

G - CHANGE GEOMETRY          C - COMPUTE/DISPLAY CURRENTS
E - CHANGE ENVIRONMENT       P - COMPUTE FAR-FIELD PATTERNS
X - CHANGE EXCITATION        N - COMPUTE NEAR-FIELDS
L - CHANGE LOADS/NETS        Q - QUIT
F - CHANGE FREQUENCY
*************************************************************************
COMMAND? N

********************** NEAR FIELDS *********************************

ELECTRIC OR MAGNETIC NEAR FIELDS (E/H) ? E

FIELD LOCATIONS(S):
   X-COORDINATE (M): INITIAL, INCREMENT, NUMBER ? 0,2,11
   Y-COORDINATE (M): INITIAL, INCREMENT, NUMBER ? .1,.2,15
   Z-COORDINATE (M): INITIAL, INCREMENT, NUMBER ? 0,0,1

CHANGE POWER LEVEL (Y/N) ? Y

NEW POWER LEVEL (WATTS) ? 1.0E3
```

The reflector of this type of antenna may be wire grids or metal sheets necessitating a choice between GTD or thin-wire codes. For the reflector dimensions of this example, the 300-segment limitation of NEC would be easily exceeded because the spacing between wires should be less than 0.1 λ according to Reference 19, p. 29-21. GTD is the logical choice; however, if several radiators are prescribed (which is not the case here) computation time becomes important (see Reference 27, p. 4).

Analysis of Results

E-field intensity as a function of azimuth ϕ angle was plotted for four distances measured from the apex of the reflector (inset, Figure 4-3). Because the corner reflector has bilateral symmetry, only half (45°) of the included angle of 90° was plotted. All intensities were normalized to the highest value of the nearest chosen distance of 2 λ. As with the on-axis analysis of the corner reflector, the off-axis curves apply at any frequency and power input for the antenna dimensions shown.

The normalized curves are useful in revealing how the near-field of a corner reflector changes when the s-parameter (dipole-to-apex distance) is moved from 0.5 λ of the on-axis analysis (inset, Figure 3-10) to 1.18 λ. This alters the single far-field mainlobe to a bifurcated lobe (see Reference 19, p. 17-4). Except for the shortest distance of 2 λ, the near-field intensity also exhibits double-lobing, albeit a shallow one.

The NEC-BSC model and its output can be verified from a plot in Reference 7, Part I, pp. 7-29 and 7-30, at the distance of 12.4 λ. Their measured data for 12.4 λ are plotted as a dotted line in Figure 4-3. Agreement is good with computed values for all azimuth angles. Note that the measurements also tend toward a shallow double lobe.

Procedures for Implementing a NEC-BSC model of a Corner Reflector

The complete NEC-BSC input data are listed in Table 4-2. Following the comment lines CM and CE, frequency FR and units of geometry UN and US are entered. The next inputs are the dipole geometry and excitation SG, and the reflector plate geometry PG. Then the near-zone coordinates are specified PN followed by the execute code XQ and end-program EN lines.

The preceding example was chosen to be nearly identical to EXAMPLE 5 [ibid] for instructional purposes. This makes the input and output data for the altered and unaltered examples easy to compare.

A first-time user will welcome NEC-BSC's exceptionally complete printed documentation. The user's manual provides several diverse tutorial examples with directly executable input lines. All examples have graphical comparisons of computer output and measurement data.

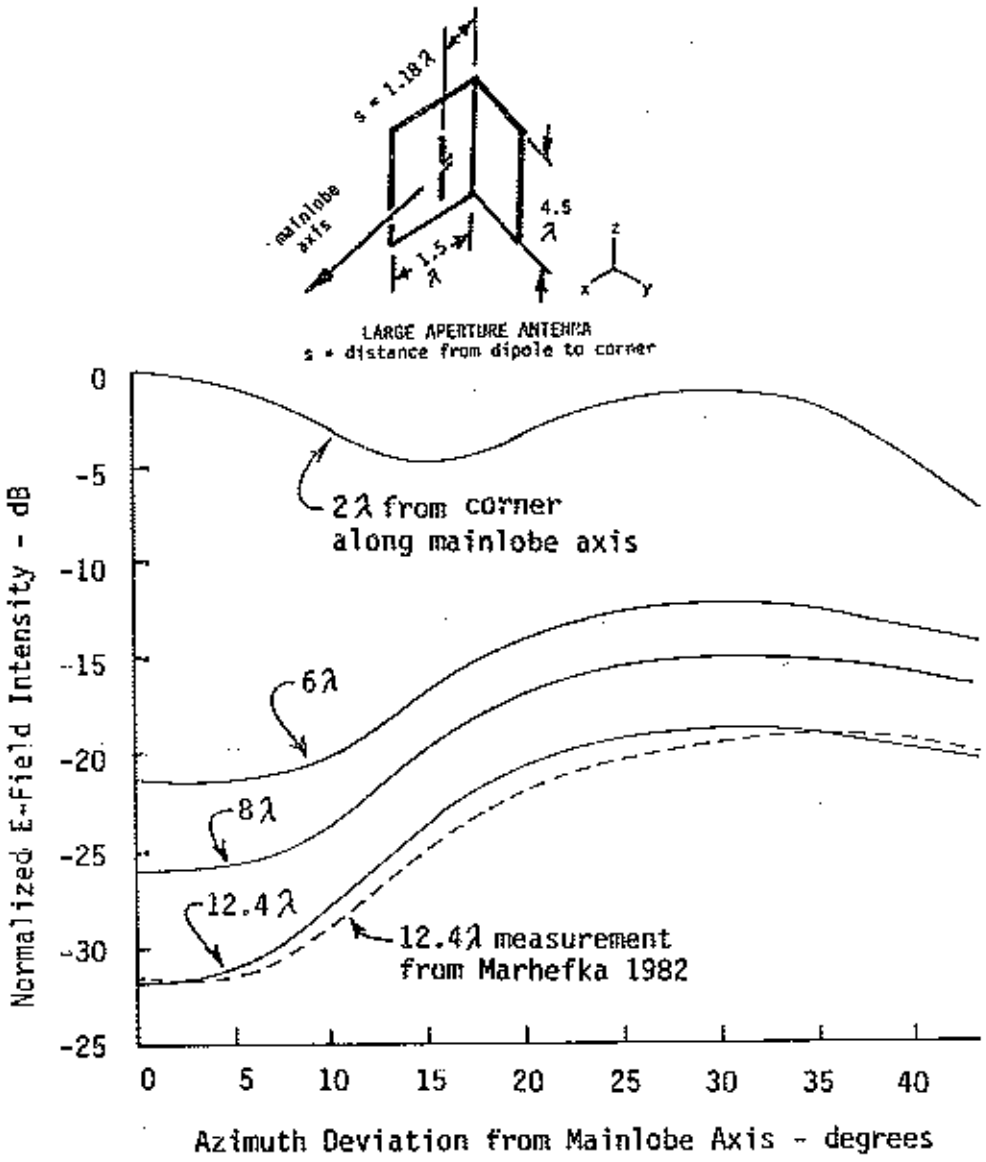

Figure 4-3. Off-axis near E-field intensity vs azimuthal angle for several distances from the radiator. 90° large-aperture corner reflector, freespace.

TABLE 4-2

INPUT DATA FOR NEC-BSC MODEL OF A 90-DEG CORNER REFLECTOR

```
CM: 90-DEG CORNER REFLECTOR
CM: NEAR ZONE, H-PLANE FIELD INTENSITY
CE: s = 1.18 LAMBDA, DIST. = 5.92 IN.

FR: FREQUENCY IN MHZ
3.985

UN: UNIT OF GEOMETRY - INCHES
3

US: UNIT OF SOURCE - INCHES
3

SG: SOURCE: LOCATION, TYPE, EXCITATION
3.5,0.,0.
0.,0.,90.,0.
-2,1.5,0.
1.,0.

PG: PLATE GEOMETRY - ONE SURFACE
4,0
0.,0.,-6.5
0.,0.,6.5
3.36,-3.36,6.5
3.36,-3.36,-6.5

PG: PLATE GEOMETRY - ONE SURFACE
4,0
0.,0.,6.5
0.,0.,-6.5
3.36,3.36,-6.5
3.36,3.36,6.5

PN: NEAR ZONE SPECIFICATIONS
0.,0.,0.
0.,0.,90.,0.
F
5.92,90.,0.
0.,0.,1.
46

XQ: EXECUTE CODE

EN: END PROGRAM
```

REFERENCES

1. NTIA, *Manual of Regulations and Procedures for Federal Radio Frequency Management*," U.S. Department of Commerce, National Telecommunications and Information Administration, Washington, D.C., Revised May 1988.

2. Farrar, A., and E. Chang, "*Procedures for Calculating Field Intensities of Antennas*," NTIA Report TM-87-129, U.S. Department of Commerce, September 1987.

3. Calhoon, E., and H.K. Kobayashi, "*Antenna Field Intensity (AFI) Program*," NTIA, Annapolis, unpublished.

4. Stutzman, W.L., and G.A. Thiele, "*Antenna Theory and Design*," J. Wiley & Sons, New York, N.Y. 1981.

5. Adams, A.T., Baldwin, T.E., and D.E. Warren, "*Near Fields of Thin-Wire Antennas-Computation and Experiment*," IEEE Transactions on Electromagnetic Compatibility, vol. EMC-20, no. 1, pp. 259-266, February 1978.

6. Logan, J.C., and J.W. Rockway, "*The New MININEC (Version 3): A Mini-Numerical Electromagnetic Code*," Naval Oceans Systems Command, San Diego, CA 92152, NOSC TD 938, September 1986.

7. Marhefka, R.J., and W.D. Burnside, "*Numerical Electromagnetic Code - Basic Scattering Code NEC-BSC (Version 2) Part I: User's Manual and Part II: Code Manual*," The Ohio State U. ElectroScience Laboratory, Dept. of Electrical Engineering, Columbus, OH, 43212, December 1982.

8. Li, S.T., J.W. Rockway, J.C. Logan, and D.W.S. Tam, "*Microcomputer Tools for Communications Engineering*," Artech House, Inc., Dedham, MA, 1983.

9. Campbell, D.V., "*Personal Computer Applications of MININEC*," IEEE Antennas and Propagation Newsletter, pp. 5-9, February 1984; "*MININEC Applications Guide*," Applied Computational Electromagnetics Society Newsletter, pp. 21-28, February 1986.

10. Burke, G.J. and A.J. Pogio, "*Numerical Electromagnetics Code (NEC) - Method of Moments, Volume 2*," NOSC Naval Oceans Systems Center, San Diego, CA, NOSC-TD 116, January 1981.

11. Burnside, W.D., "*Computer Modeling of Electromagnetic Problems Using the Geometrical Theory of Diffraction*," IEEE International Symposium on Electromagnetic Compatibility, Washington, D.C., July 13-15, 1987, pp. 312-316.

12. Burnside, W.D., R.C. Rudduck, and R.J. Marhefka, "*Summary of GTD Computer Codes Developed at the Ohio State University*," IEEE Transactions on Electromagnetic Compatibility, vol. EMC-22, no. 4, pp. 238-243, November 1980.

13. Siarkiewicz, K.R., "*GEMACS - An Executive Summary*," Applied Computational Electromagnetics Society (ACES) Newsletter, vol. 2, no. 1, pp. 124-136, May 1987.

14. Bickmore, R.W. and R.C. Hansen, "*Antenna Power Densities in the Fresnel Region*," Proceeding IRE (IEEE), pp. 2119-2120, December 1959.

15. Balanis, "*Antenna Theory, Analysis and Design*," Harper and Row, Inc., New York, NY, 1982.

16. Thiele, G.A., E.P. Ekelman, and L.W. Henderson, "*On the Accuracy of the Transmission Line Model for Folded Dipole*," IEEE Transactions Antennas and Propagation, vol. AP-28, No. 5, pp. 700-703, Sept. 1980.

17. Tilston, W.V., "*On Evaluating the Performance of Communications Antennas*," IEEE Communications Magazine, pp. 18-27, Sept. 1981.

18. Kalhor, H.A. and A.R. Mallahzadeh, "*Analysis of a Folded Dipole Antenna Mounted on a Cylindrical Metallic Mast*," IEEE Transactions on Antennas and Propagation, vol. AP-34, no.1, pp. 99-103, Jan. 1986.

19. Johnson, R.C. and H. Jasik, "*Antenna Engineering Handbook*," McGraw-Hill Book Co., New York, N.Y. 1961.

20. Jessop, G.R., "*VHF/UHF Manual, Fourth Edition*," Radio Society of Great Britain, Hertfordshire, England, 1983.

21. Kandoian, A.G., "*Three New Antenna Types and Their Applications*," Procedures IRE (IEEE), vol. 34, pp. 70W-75W, February 1946.

22. Collins Radio Company, "*Collins High-Frequency Antennas/Selection/Applications*," Research Division, Collins Radio Co., Cedar Rapids, Iowa, May 1, 1961.

23. Wolf, E.A., "*Antenna Analysis*," J. Wiley & Sons, New York, N.Y., 1966.

24. Kobayashi, H.K., "*Modeling a Receiving MF-HF Phased Antenna Array: Numerical Computation vs Field Measurements*," Proceedings IEEE Region 1 Workshop on Electromagnetic Field Computation, Schenectady, NY, Volume II, pp. E-30 - E-34, October 20-21, 1986.

25. Ryan, Jr, C.E., F.L. Cain, J.J.H. Wang, B.J. Cown, and W.P. Cooke, IEEE Transactions on Electromagnetic Compatibility, vol. EMC-22, no. 4, pp. 244-255, November 1980.

26. Koh, W.J., "*Radiation Hazard Evaluation for a High Power Mobile Electromagnetic Radiation Weapon Using the Numerical Electromagnetic Code*," M.S. Thesis, Naval Postgraduate School Monterey, CA, March 1987.

27. Koh, W.J. and R.W. Adler, "*Radiation Hazard Evaluation Using NEC-BSC*," Conference Proceedings 3rd Annual Review of Progress in Applied Computational Electromagnetics, Monterey, CA, March 24-26, 1987.

28. Rudduck, R.C. and Y.C. Chang "*Numerical Electromagnetic Code NEC-REF (Version 2) Part I: User's Manual*," The Ohio State U. ElectroScience Laboratory, Dept. of Electrical Engineering, Columbus, OH 43212, December 1982.

29. Siarkiewicz, K.R., "*GEMACS - An Executive Summary*," Applied Computational Electromagnetics Society (ACES) Newsletter, vol. 2, no. 1, pp. 124-136, May 1987.

FORM NTIA-29
(4-80)

U.S. DEPARTMENT OF COMMERCE
NAT'L. TELECOMMUNICATIONS AND INFORMATION ADMINISTRATION

BIBLIOGRAPHIC DATA SHEET

	1. PUBLICATION NO.	2. Gov't Accession No.	3. Recipient's Accession No.
	NTIA TM-88-135		

4. TITLE AND SUBTITLE
PROCEDURES FOR CALCULATING FIELD INTENSITIES OF ANTENNAS, PHASE II

5. Publication Date
SEPTEMBER 1988

6. Performing Organization Code
NTIA/OSM/SEAD

7. AUTHOR(S)
Herbert K. Kobayashi

8. PERFORMING ORGANIZATION NAME AND ADDRESS
National Telecommunications and
Information Administration
179 Admiral Cochrane Drive
Annapolis, Maryland 21401

9. Project/Task/Work Unit No.
9018171

10. Contract/Grant No.

11. Sponsoring Organization Name and Address
U.S. Department of Commerce/NTIA
179 Admiral Cochrane Drive
Annapolis, Maryland 21401

12. Type of Report and Period Covered
TECHNICAL MEMORANDUM

13.

14. SUPPLEMENTARY NOTES

15. ABSTRACT *(A 200-word or less factual summary of most significant information. If document includes a significant bibliography or literature survey, mention it here.)*

This technical report augments the procedures given in NTIA TM-87-129 for calculating the near-field power density of commonly encountered linear (wire) and aperture antennas. Ninety-seven percent of the 100,000 antennas in the Government Master File (GMF) are covered by the two reports. The categories of linear and aperture antennas are clarified as a prelude to selecting an antenna for mainbeam on-axis calculation, and choosing a numerical computer code for an off-axis situation.

Guidance for on-axis analysis of more than 10 antenna types not covered in TM-87-129 is provided. Calculations using simple formulas and normalized intensity vs distance graphs are made clear by sample calculations for all antenna types.

Procedures and examples of off-axis analysis are provided in selecting and applying an appropriate numerical computer code to an arbitrary linear or aperture antenna.

16. Key Words *(Alphabetical order, separated by semicolons)*

Antenna Gain Calculation; Linear (Wire) and Aperture Antennas;

Near-Field Power Density (Intensity); Numerical Computer Programs (Models)

17. AVAILABILITY STATEMENT	18. Security Class. *(This report)*	20. Number of pages
☒ UNLIMITED.	UNCLASSIFIED	55
☐ FOR OFFICIAL DISTRIBUTION.	19. Security Class. *(This page)* UNCLASSIFIED	21. Price:

☆U.S. Government Printing Office: 1988—670-485/60129